

STUDIES ON THE CHEMICAL AND PHYSICAL PROPERTIES OF
NATIVE, IMMOBILIZED AND COBALT-SUBSTITUTED RUBREDOXIN

A THESIS

Presented to

The Faculty of the Division of Graduate Studies

by

Jong-Yuan Kuo

In Partial Fulfillment
of the Requirements for the Degree
Doctor of Philosophy in the
School of Chemistry

Georgia Institute of Technology

January, 1978

STUDIES ON THE CHEMICAL AND PHYSICAL PROPERTIES OF
NATIVE, IMMOBILIZED AND COBALT-SUBSTITUTED RUBREDOXIN

Approved:

[Handwritten signature]

Date approved by Chairman: 1/20/78

To my parents and wife

ACKNOWLEDGEMENTS

I wish to express my sincere appreciation to my thesis advisor, Dr. Sheldon W. May, for his wise guidance, patience, constant encouragement and enthusiastic support. I have thoroughly appreciated our relationship. Dr. Ronald Felton was most helpful and informative on magnetic circular dichroism. The data supplied by Mr. Duncan Cheung on Laser-Raman spectra is greatly appreciated, as is the gas chromatography data supplied by Mr. Mike Steltenkamp. I would also like to thank Dr. Carole Hall for many valuable discussions. The weekly literature seminars by the members of Dr. May's research group were also pleasant as well as educational.

Financial assistance from the Georgia Institute of Technology, the National Science Foundation, the Research Corporation, and the National Institutes of Health is gratefully acknowledged.

Finally, I am indebted to my parents overseas for their constant support and encouragement over many years, and to my wife, Alison, for her continued help, affection, and understanding.

TABLE OF CONTENTS

	Page
ACKNOWLEDGEMENTS	iii
LIST OF TABLES	vi
LIST OF ILLUSTRATIONS	vii
ABBREVIATIONS	ix
SUMMARY	xi
Chapter	
I. INTRODUCTION	1
Oxygenases	
Rubredoxin	
Rubredoxin Reductase	
II. EXPERIMENTAL	15
Materials	
Chemicals	
Organism	
Methods	
Fermentation	
Resting Cell Assay for Epoxide Formation	
Assay of Rubredoxin by Cytochrome c Reduction	
Assay Based on Reduction of the Rubredoxin Chromophore	
Protein Determinations	
Isolation of Rubredoxin	
Isolation of Spinach Reductase	
Preparation of Alkyl and ω -Aminoalkyl Sepharose	
Isolation of Rubredoxin Reductase	
Disc Electrophoresis	
Isoelectrofocusing	
Preparation of Immobilized Rubredoxin	
Amino Acid Analysis	
Spectrophotometric Measurement of Immobilized Rubredoxin	
Anaerobic Reduction of Immobilized Rubredoxin	
Reduction Potential Measurement of Immobilized Rubredoxin	
Reconstitution of Immobilized Rubredoxin	

Chapter	Page
II. Stability Comparison of Soluble and Immobilized Rubredoxin Preparation of Aporubredoxin Preparation of Reconstituted Rubredoxin Natural and Magnetic Circular Dichroism Measurement Laser-Raman Spectra Measurement Difference Spectra Measurement Sulfhydryl Titrations	
III. RESULTS	51
Fractions From First DEAE Chromatography Affinity Chromatography of Rubredoxin Reductase Characteristics of Isolated Rubredoxin Preparation of Immobilized Rubredoxin Spectral Properties of Immobilized Rubredoxin Redox Properties of Immobilized Rubredoxin Guanidine HCl Denaturation of Immobilized and Soluble Rubredoxin Iron Removal and Reconstitution of Immobilized Rubredoxin Reconstitution of Soluble Rubredoxin Spectral Properties of Cobalt Rubredoxin Natural and Magnetic Circular Dichroism Spectra Laser-Raman Spectra Difference Spectra Electron Transfer Activity Stability Toward Chelating and Denaturing Reagents Sulfhydryl Titrations Oxidation Reduction Properties of Cobalt Rubredoxin	
IV. DISCUSSION	95
REFERENCES	110
VITA	117

LIST OF TABLES

Table	Page
1. Composition of P-1 Media (Per Liter)	17
2. Characteristics of Fractions From First DEAE Chromatography	26
3. Preparation of Rubredoxin from 1 kg Cells . . .	30
4. Data of Amino Acid Analysis	41
5. Coupling Yields in Preparation of Immobilized Rubredoxin	57
6. Reduction Potential of Immobilized Rubredoxin .	68
7. Iron Dissociation and Reconstitution with Immobilized Rubredoxin	72
8. Comparison of Iron and Cobalt Binding to Aporubredoxin	74

LIST OF ILLUSTRATIONS

Figure	Page
1. Schematic Diagram of <i>P. oleovorans</i> Rubredoxin and Model for Iron-Binding Sites	10
2. A Possible Evolutionary Pathway of the Rubredoxin Gene in the Rubredoxin Containing Organisms . .	12
3. Growth Curve of <i>P. oleovorans</i> in the Fermentor	20
4. DEAE Chromatography of 30-60% Ammonium Sulfate Fractionation From Sonicate Extract	25
5. Sephadex G-75 Chromatography of Rubredoxin Concentrate From DEAE Elution	27
6. Second DEAE Chromatography of Rubredoxin From Sephadex G-75 Elution	28
7. Second Sephadex G-75 Chromatography of Rubredoxin From Second DEAE Elution	29
8. DEAE Chromatography of 35-75% Acetone Fractionation From Spinach Homogenates	32
9. Sephadex G-50 Chromatography of 40-65% Ammonium Sulfate Fractionation From DEAE Elution	34
10. DEAE Chromatography of Yellow Eluate From Sephadex G-50 Chromatography	35
11. Affinity Chromatography of Rubredoxin Reductase	53
12. Comparative Spectra of Soluble and Immobilized Rubredoxin	60
13. Spectral Changes Upon Anaerobic Reduction of Immobilized and Soluble Rubredoxin.	64
14. Rubredoxin-Dependent Reduction of Cytochrome c.	66
15. Stability of Soluble and Immobilized Rubredoxin	70
16. Absorption Spectrum of Cobalt Rubredoxin	76

Figure	Page
17. MCD and CD Spectra of Cobalt Rubredoxin	78
18. Difference Spectra of Rubredoxin and Reductase	81
19. Comparative Electron Transfer Activities of (2Fe)-, (2Co)-, PHMB-modified Co-, and Aporubredoxin	83
20. Stability Comparison of (2Fe)- and (2Co)- Rubredoxin	86
21. Reaction of Excess Aldrithiol-4 with (2Fe)- and (2Co)-Rubredoxin	89
22. Reaction of Quantitative Amounts of PHMB with (2Fe)- and (2Co)-Rubredoxin	91
23. The Time Course of the Reactions with Aldrithiol-4	93

ABBREVIATIONS

<u>Abbreviation or Trivial Name</u>	<u>Systematic Name</u>
Aldrithiol-4	4,4'-dithiodipyridine
Aporubredoxin	Rubredoxin with no metal atom
CD	Circular Dichroism
CM	Carboxymethyl
(2Co)-Rubredoxin or Cobalt Rubredoxin	Rubredoxin containing two g-atoms of cobalt per mole of protein
D.O.	Dissolved oxygen
DEAE, or DE-52	Diethylaminoethyl
Dithizone	Diphenylthiocarbazone
DTNB or Ellman's reagent	5,5'-Dithiobis(2-nitrobenzoic acid)
$E_{m,7}$	Midpoint potential at pH 7.0, 25°.
EDTA	Ethylenediaminetetraacetate
EPR	Electron Paramagnetic Resonance
(1Fe)-rubredoxin	Rubredoxin containing one g-atom of iron per mole of protein
(2Fe)-rubredoxin	Rubredoxin containing two g-atoms of iron per mole of protein
g	Gravitational constant
ω -Hydroxylase	Alkane, reduced-rubredoxin:oxygen 1-oxidoreductase (EC 1.14.15.3)
Immobilized Rubredoxin or Rubredoxin conjugate	Rubredoxin, covalently attached to a Sepharose 4B support
Indigo carmine	3,3'-dioxo- $[\Delta^2, \Delta^2'$ biindoline] 5,5'-disulfonic acid

<u>Abbreviation or Trivial Name</u>	<u>Systematic Name</u>
NADH	Dihydrodiphosphopyridine nucleotide
NADPH	Dihydrotriphosphopyridine nucleotide
O.D.	Optical density
PHMB	<u>p</u> -Hydroxymercuribenzoate
Rubredoxin	Unless state otherwise, rubredoxin from <u>P. oleovorans</u> , may indicate soluble iron, cobalt or modified rubredoxin
Rubredoxin Reductase	Reduced-NAD:rubredoxin oxidoreductase from <u>P. oleovorans</u> (EC 1.6.7.2)
Spinach Reductase	Reduced-NADP:ferredoxin oxidoreductase (EC 1.6.99.4)
Tris	Tris(hydroxymethyl) aminomethane
$[\theta]_M$	Magnetic ellipticity
$[\theta]_\lambda$	Molar ellipticity
ϵ_M	Molar extinction coefficient
λ	Wavelength

SUMMARY

Rubredoxin, an iron-sulfur protein and one of the three components of the epoxidation/hydroxylation system of Pseudomonas oleovorans was isolated by a new procedure and examined with respect to a number of chemical and physical properties. The protein was immobilized by attachment to CNBr-activated Sepharose 4B. Since this represents the first example of a water-insoluble derivative of an enzyme of this type, the spectral characteristics, physical stability, oxidation-reduction properties and ability to complex with, and accept electrons from, a flavoprotein reductase were examined in order to allow comparison with those of the soluble enzyme. In the course of these studies, the flavoprotein, rubredoxin-reductase, was also isolated by a novel procedure which employs hydrophobic chromatography.

The native iron atoms in the metal chromophores of rubredoxin were successfully replaced by cobalt using a newly developed reconstitution process. The resultant Co(II)-rubredoxin shows distinct chemical and physical properties including UV-visible, MCD, CD, and Laser-Raman spectra, oxidation-reduction ability, interaction with chelating and thiol reagents, etc., which are different from those of the native iron-rubredoxin.

CHAPTER I

INTRODUCTION

Oxygenase

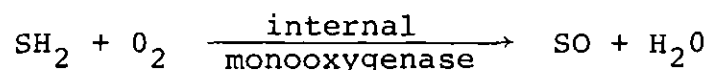
Oxygenases are among the most ubiquitous and metabolically significant of all enzymes. They are enzymes which incorporate molecular oxygen directly into organic molecules, and do so with high efficiency and selectivity. These enzymes are capable of converting alkanes to alcohols or olefins to epoxides; cleaving aromatic rings or oxidizing their substituents; oxidatively demethylating O- or N-methyl groups; and hydroxylating aromatic or polycyclic hydrocarbons and steroid derivatives (1). Thus, oxygenases are essential for key steps in biosynthesis, interconversion, and degradation of aromatic acids, lipids, sugars, porphyrins, vitamins and hormones. Oxygenases are particularly involved in the degradation of drugs and foreign substances and thus in mechanisms of cytotoxicity, mutagenicity, carcinogenicity and tissue necrosis. Yet, the molecular basis for the action of these enzymes, their metabolic patterns and their associated electron transport proteins are not well-understood. Such an understanding would be helpful in the design of new drugs and the development of model enzyme systems.

Two subclasses of oxygenases may be defined (2). Dioxygenases catalyze the incorporation of both atoms of

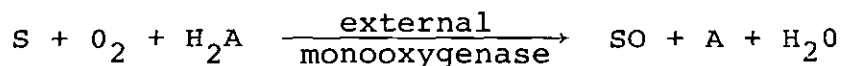
molecular oxygen into a molecule of substrate (S):



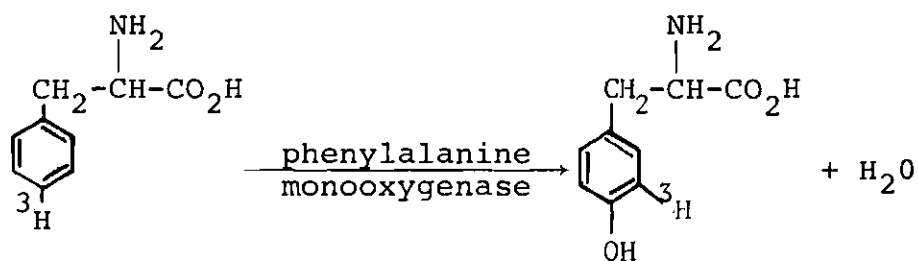
The major reaction catalyzed is the cleavage of an aromatic double bond. It has been tacitly assumed that iron in the active center of these oxygenases plays a role in the activation of oxygen. In addition, a ternary complex with substrate is usually formed. On the other hand, monooxygenases catalyze the incorporation of a single atom of oxygen into the substrate concomitant with the reduction of the other oxygen atom to water by the electrons derived either from substrate (called "internal monooxygenases"):



or from electron donor H_2A (called "external monooxygenases"):



The major reactions catalyzed are the hydroxylation of aromatic and aliphatic compounds, as well as epoxide formation (see below), dealkylation, decarboxylation, deamination, and N- or S- oxide formation. It has recently been discovered that the so-called "NIH shift" is catalyzed by monooxygenases; that is, an intramolecular migration of proton concomitantly occurs during the enzymatic hydroxylation of aromatic substrates (3).



The presence of physiologically important oxygenases in animals is generally confined to specialized organs and tissues, and the amounts of oxygenases are rather limited. On the other hand, a number of oxygenases in microorganisms are inducible and therefore bacteria serve as a much better source of these enzymes in quantities needed for laboratory studies and make possible a thorough analysis of their mechanisms of action. Almost all the oxygenases which have so far been purified were obtained from aerobic bacteria, such as *Pseudomonas*, *Mycobacteria* and *Norcardia*. At present, studies are focused on two related aspects of the general problem - 1) the nature of the "active oxygen" species, and 2) the mechanism by which it is formed. For example, the intermediacy of singlet oxygen has been of much concern in many biological systems.

Since monooxygenase reactions involve both electron transfer and oxygen insertion steps, Hamilton proposed that an "oxenoid" species is generated in these reactions by transfer of the two electrons to oxygen prior to, or concurrent with, transfer of an oxygen atom to the substrate (4), similar to the insertion of carbene or nitrene into C-H and C=C

bonds (5). However, the structure of an actual enzymatic oxenoid intermediate has never been identified (6), though it probably is involved in some organic reaction, e.g., the peracid epoxidation of olefins.

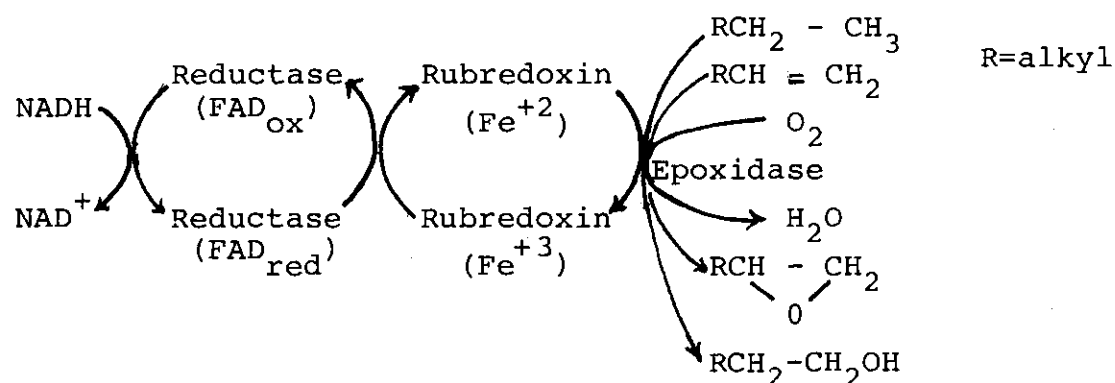
This discussion will be confined to an enzymatic system of Pseudomonas oleovorans, which participates in the epoxidation of the terminal double bonds in olefins.

The enzymatic system involved was first isolated by Coon and coworkers (7-16) and shown to consist of three protein components - rubredoxin, a NADH-rubredoxin reductase, and " ω -hydroxylase." Rubredoxin is a non-heme iron-sulfur protein of molecular weight 19,000, which is capable of binding either one or two iron atoms per molecule (8, 9, 11). The reductase is a flavoprotein of molecular weight 55,000 (12, 15). The " ω -hydroxylase" has proved to be exceedingly difficult to purify, but it is apparently a non-heme iron protein (10, 16). In the presence of NADH and molecular oxygen, this enzyme system catalyzes the hydroxylation of the terminal methyl groups of alkanes and fatty acids, as established by Coon and coworkers (7).

Recently, May and coworkers found that this same enzyme system also converts terminal olefins to the corresponding terminal epoxides (17-26). The epoxidation reaction requires the presence of all three protein components as well as NADH and molecular oxygen. A 1:1:1 stoichiometry was obtained between the amount of epoxide product formed, the amount of

NADH oxidized and the amount of oxygen consumed (17, 18), which is diagnostic characteristic of reactions catalyzed by mixed function oxidases (scheme I).

Scheme I:



The substrate 1-octene, which contains both a terminal methyl group and a terminal double bond, is converted to both 7-octene-1-ol and 1,2-epoxyoctane. However, 1,7-octadiene which does not have a terminal methyl group, is converted to 7,8-epoxy-1-octene, and more than 90% of the epoxide product is the R(+) isomer. This high stereospecificity requires that the addition of oxygen to the incipient asymmetric carbon of octadiene occur exclusively from the si-si face of the double bond (21). Furthermore, this R(+) isomer can be oxidized to 1,2;7,8-diepoxyoctane, and more than 80% of the diepoxide produce is the (R,R)-(+) isomer. However, a comparative analysis with the configuration of diepoxide produced enzymatically from racemic (R,S)-7,8-epoxy-1-octene has revealed that the configuration of the preformed asymmetric

epoxide group profoundly affects the stereochemical consequences of oxygen insertion into a double bond at the other end of molecule (26).

The exact relationship between the hydroxylation and epoxidation reactions is not completely clear. They are both inhibited by cyanide, affected similarly by pH, and show the same cofactor selectivities; thus, epoxidation and hydroxylation activities are probably inseparably associated with the same active site of the oxygenase, which does not contain P-450. Since P-450 has been found in extracts of an octane-utilizing *Corynebacterium* (27), camphor methylene hydroxylase system of *P. putida* (28), steroid 11 β -hydroxylase system of bovine adrenocortical mitochondria (29, 30) and many liver microsomal systems which catalyze the oxidation of steroids, fatty acids, drugs, aromatic compounds and xenobiotics (31, 32), an unusual mechanism of oxygen activation in *P. oleovorans* system is possible.

Rubredoxin

The number of metalloproteins, especially metallo-enzymes, which have been discovered and well characterized, has increased exponentially since about 1960. Among these, iron proteins are of the most interest to biochemists, due to the participation of iron in many transport and catalytic processes. If the iron is coordinated to sulfur, either from cysteine or from inorganic sulfur, then the protein is called an "iron-sulfur protein" (1a). According to the IUPAC-IUB (33),

the various iron-sulfur proteins are classified to four categories: (1) ferredoxins; (2) high potential iron-sulfur proteins (HPIP); (3) conjugated iron sulfur proteins; and (4) rubredoxins. The latter have been obtained from both anaerobic and aerobic organisms. Examples of anaerobes containing rubredoxin are Clostridium pasteurianum (34, 35), C. butyricum (36), C. stricklandii (37), Desulfovibrio desulfuricans (38), D. gigas (39), Micrococcus aerogenes (40), Peptostreptococcus glycinophilus (41), and P. elsdenii (42). The only aerobe known to contain rubredoxin is Pseudomonas oleovorans.

Rubredoxins contain no acid-labile sulfur, but rather an iron atom ligated to four cysteine residues. The enzymes from anaerobic species contain one such iron per molecule. Carboxymethylation of these residues by iodoacetate only occurs after iron has been completely removed. The rubredoxins have molecular weights of around 6,000 daltons and are characterized by an abundance of aspartate and glutamate residues, and the absence of both arginine and histidine, in the amino acid composition. The crystal structure of the rubredoxin from C. pasteurianum has been determined to 1.5 Å resolution (43). The most striking structural feature is tetrahedral coordination of the metal ion by four mercaptide sulfur atoms from cysteines with S-Fe bond lengths varying from 2.05 to 2.34 Å. The molecule consists of an irregularly folded polypeptide chain which contains an appreciable amount

of antiparallel sheet structure but no alpha helix. Upon reduction of the iron from ferric to ferrous ($E' = -57\text{mv}$), the coordination geometry is still tetrahedral. The oxidized protein exhibits a strong EPR singal with $g = 4.0\sim 4.3$. This resonance is typical of Fe^{+3} subjected to relatively small distortions. For the reduced proteins, containing Fe^{+2} with an even number of electrons, no EPR was observed. The laser-Raman spectrum exhibits two lines at 365 and 311 cm^{-1} , which correspond to two symmetric stretching modes of the Fe-S_4 tetrahedron (44). The visible spectra show that all the rubredoxins so far studied have the same absorption patterns with maxima around 480 and 380 nm . They all result from an $\text{S}^- \rightarrow \text{Fe}^{+3}$ charge transfer transition (45). Upon reduction, the lowest energy transition is observed at 320 nm . The apoprotein of this iron-sulfur protein can be prepared by trichloroacetic acid precipitation. While it has been shown that rubredoxin can replace ferredoxin as an electron carrier in certain systems, the exact role of rubredoxin in anaerobic species is not understood. Thus far many analogous complexes involving metal-thiolate ligation have been synthesized and investigated (46-51).

On the other hand, the physiological function of rubredoxin from the aerobe *P. oleovorans*, is well-established. It mediates electrons transfer between NADH-rubredoxin oxidoreductase and ω -hydroxylase, and thus is required for hydroxylation (7-16) and epoxidation (17-26) with a stoichio-

metry typical of monooxygenases. Although alkyl hydroperoxides could be reduced to alcohols in the presence of NADH, rubredoxin and NADH:rubredoxin reductase, attempts to identify an alkyl hydroperoxide as a free or enzyme-bound intermediate in the hydroxylation reaction have so far proved unsuccessful (14).

The molecular weight of rubredoxin from P. oleovorans is about 19,000, and it is composed of 174 amino acids with two iron binding sites. The amino acid sequence (13) and metal sites are shown schematically in Figure 1 (11). The protein contains a single methionine residue and 10 cysteine residues, and unlike the rubredoxins from anaerobes, it also contains histidine and arginine. The two iron binding sites, known to be located at either end of the protein chain, appear to be two noninteracting $\text{Fe}[\text{S-Cys}]_4$ sites with a highly asymmetric environment as reflected in the ORD and CD spectra (9). However, the iron bound at the N-terminal site is vastly more labile than that at the C-terminal site. On a molar basis, however, (1Fe)- and (2Fe)- rubredoxin function equally well as electron carrier in ω -hydroxylation system, indicating that only one iron atom per molecule is necessary and that the addition of a second iron atom apparently does not enhance the activity. Chemical cleavage of aporubredoxin at the single methionine followed by reconstitution with iron gives a C-terminal fragment with 30% of the activity of the original protein in octane hydroxylation, while the N-terminal fragment is inactive. Interestingly, residues 1-54 and 119-174 were found to be two homologous sections, which were also homologous

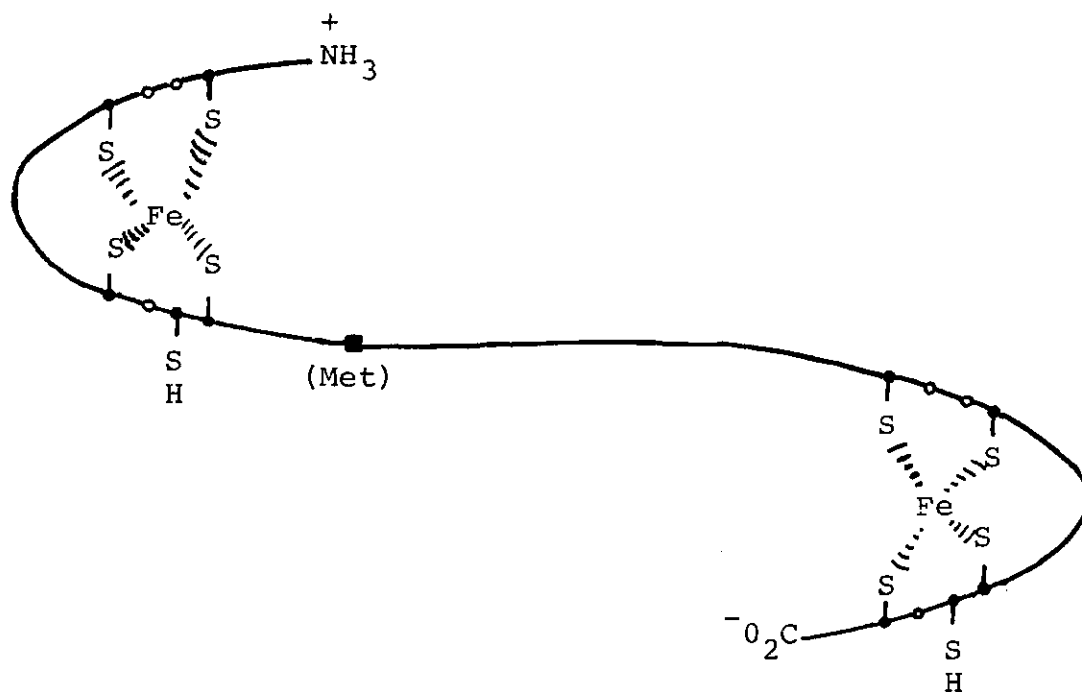


Figure 1. Schematic Diagram of *P. oleovorans* Rubredoxin and Model for Iron Binding Sites(11).

with the anaerobic type of rubredoxin (13). According to evolutionary theory, the aerobe would be more advanced than the anaerobe. An approximate phylogenetic tree is shown in Figure 2 (13).

Despite the similarities in many of their physical and chemical properties, rubredoxins from anaerobes appear not to substitute for the P. oleovorans enzyme in hydroxylation (8, 9), even though they do accept electrons from the P. oleovorans reductase (12). Iron sulfur proteins of the ferredoxin type ($2\text{Fe}-2\text{S}^*$), e.g., adrenodoxin from the adrenocortical mitochondria system or putidaredoxin from P. putida system, can neither accept electrons from P. oleovorans reductase nor substitute for rubredoxin in hydroxylation. Taken together, these facts suggest that P. oleovorans rubredoxin, with its unique functionalities and structural features, may not only function in electron transport to the "oxygenase," but that it may also participate more directly in the binding and activation of oxygen. Oxygen binding would require reorientation of the sulfur ligands, presumably toward tetragonal geometry. Of course, the participation of another non-heme iron moiety in the "epoxidase/hydroxylase" is also possible in this step, since the hydroxylase contains non-heme iron (10).

Rubredoxin Reductase (EC 1.6.7.2)
(NADH:Rubredoxin Oxidoreductase)

This reductase contains 1 mole of FAD per mole of protein and has a molecular weight of 55,000 with a high content

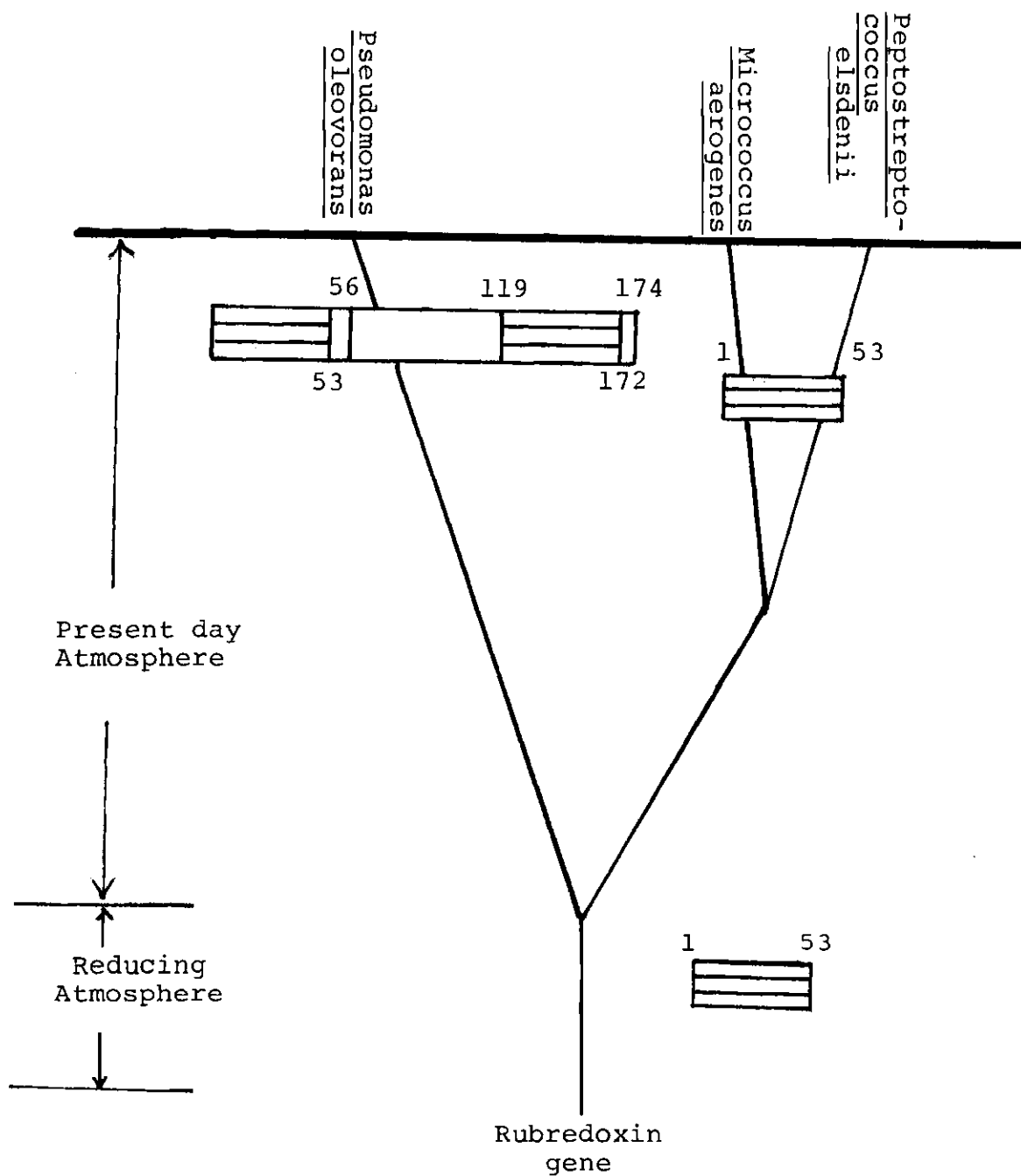


Figure 2. A Possible Evolutionary Pathway of the Rubredoxin Gene in the Rubredoxin Containing Organisms(13).

of hydrophobic residues, particularly leucine, isoleucine and valine. The formation of a charge transfer complex between the reduced flavoprotein and NAD^+ has been detected (15). Examination of the interaction between reductase and rubredoxin by both spectrophotometric and fluorimetric techniques shows that these two components form a 1:1 complex with a dissociation constant at $0.21 \mu\text{M}$, but that they dissociate easily at high ionic strength. The reductase transfers electrons to rubredoxin of P. oleovorans as well as to rubredoxins of anaerobic bacteria. In contrast to the nonspecificity of spinach ferredoxin-NADP reductase, it is inactive with non-heme iron proteins containing acid-labile sulfide, such as spinach ferredoxin, putidaredoxin, and adrenodoxin. In the presence of the reductase and rubredoxin, electrons are transferred from NADH to cytochrome c (12). Although hydroxylations catalyzed by a reconstituted liver microsomal system containing cytochrome P-450, NADPH-cytochrome P-450 reductase and phosphatidylcholine are supported by a superoxide generating system and inhibited by superoxide dismutase (15), the cytochrome c reduction catalyzed by P. oleovorans rubredoxin reductase does not appear to involve superoxide in that it is not inhibited by the dismutase. However, the oxygen-dependent oxidation of epinephrine in the presence of NADH, rubredoxin and reductase does involve the participation of superoxide (19).

Despite its unique functionality, because the instability of the reductase has interfered with its purification, this

enzyme was usually replaced by spinach ferredoxin-NADP reductase and NADPH in hydroxylation studies by Coon's co-workers.

CHAPTER II

EXPERIMENTAL

Materials

Chemicals

Hydrocarbons and organic reagents were obtained from various sources and routinely distilled or recrystallized before use. Preswollen DEAE-cellulose (DE-52) was purchased from Whatman; Sephadex and Sepharose from Pharmacia; Bio-gel A and Chelex-100 (100-200 mesh, sodium form) from Bio-Rad; ammonium sulfate, guanidine HCl (both ultrapure), and streptomycin sulfate from Schwarz/Mann; Aldrithiol-4 (4,4'-dithiodipyridine), *m*-chloroperoxybenzoic acid, indigo carmine, 1,8-diaminooctane and *n*-octylamine from Aldrich; β -mercaptoethanol, octane, 2-octanol and 1,6-hexanediamine from Eastman; Ampholines from LKB; DNase (grade I), RNase (grade I), tetrasodium EDTA, CNBr, sucrose, β -NADPH, ferredoxin, cytochrome c (type IV) and *p*-hydroxymercuribenzoate from Sigma; Tris base, monoethanolamine, trichloroacetic acid and 1,10-phenanthroline from Fisher (all certified reagents). Spectrographically pure cobalt chloride and cobalt sulfate were obtained from Johnson Matthey, London, England. Inorganic salts were of reagent grade or better. Sulfobetaine DLH was a gift from Textilana Corp. and was purified before by chromatography on Bio-Rad AG11-A8 mixed bed ion exchange resin to

remove ionic species from the neutral material.

For reconstitution experiments all buffer solution used were pretreated either by extracting with dithizone (diphenylthiocarbazone, Fisher) in CCl_4 or by the following procedure (52): Chelex-100, which had been treated sequentially with 1M NaOH, water and 10 mM tetrasodium EDTA, was washed with distilled water which had been freed of trace metal contaminants by passage over a mixed-bed ion-exchange column. One volume of the treated Chelex was mixed with four volumes of Tris base, stirred for 30 minutes and then centrifuged to remove the Chelex. All glassware was cleaned by soaking in a bath of 2N HNO_3 overnight, followed by rinsing in deionized water.

Amino acid analyses were kindly carried out by Dr. Dirk Meyers of the Coca-Cola Research Laboratories, Atlanta, Georgia.

All growth media were autoclaved at 120° and 19 psi for 30 minutes (53); when octane was to be included, it was passed through a millipore filter and added to P-1 medium (Table 1) at the time of use. Fernbach flasks containing P-1 medium were incubated in a shaker (New Brunswick Scientific Company) operated at 300 rpm and 30° .

Organism

Pseudomonas oleovorans strain TF4-1L was used throughout the experiments. The original nutrient agar slant was washed with 5 ml of P-1 medium, and the washings were used to inocu-

Table 1. Composition of P-1 Media (Per Liter).

<u>Compound</u>	<u>Amount</u>
$(\text{NH}_4)_2\text{HPO}_4$	10.0 g
K_2HPO_4	5.0 g
Na_2SO_4	0.5 g
$\text{CaCl}_2 \cdot 2\text{H}_2\text{O}$ (66 g/l)	1.0 ml
*Salt "B"	10.0 ml
**Microelements	1.0 ml
Distilled Water	1 1

*Salt "B" composition

MgSO_4	19.4 g
$\text{FeSO}_4 \cdot 7\text{H}_2\text{O}$	2.0 g
$\text{MnSO}_4 \cdot \text{H}_2\text{O}$	1.6 g
NaCl	2.0 g
Distilled water	1 1

**Microelements composition

H_3BO_3	0.50 g
$\text{CuSO}_4 \cdot 5\text{H}_2\text{O}$	0.04 g
$\text{Na}_2\text{MoO}_4 \cdot 2\text{H}_2\text{O}$	0.20 g
$\text{ZnSO}_4 \cdot 7\text{H}_2\text{O}$	8.00 g
$\text{CoCl}_2 \cdot 6\text{H}_2\text{O}$	0.20 g
Distilled water	1 1

late a shake-flask containing octane (to 1% v/v) as substrate in 100 ml P-1 medium. Stock cultures, which were derived from the previous flask at late log phase, were maintained in sealed ampoules. Each ampoule containing 3 ml concentrated (10:1) cell suspension with 0.3 ml glycerol was stored at -40°. A master flask prepared from each ampoule and grown to maximum optical density (~16, at 660 nm) was used as inoculum for large quantities of cells grown in a 14 liter fermentor (Model 19, New Brunswick Scientific, Edison, New Jersey) equipped with dissolved oxygen and pH probes and a mechanical foam breaker.

Methods

Fermentation

An inoculum of 200 ml from the master flask described above was added to the fermentor vessel which contained 10 l P-1 medium, 100 ml sterilized octane and 10 ml polypropylene glycol as an antifoaming agent. Temperature was maintained at 30°. After the medium was flushed with air from a compressor for 30 min., the air supply was reduced to 0.7 l/min at 15 psig. The agitation speed was set at 800 rpm. The dissolved oxygen (D.O) probe was connected to a L & N recorder on which the span was set at 2 mv, and chart speed at 1 inch/hr. The initial trace of D.O. is usually set at 50% on the chart paper. After 10 hrs. of growth on this amount of octane, the D.O. becomes completely exhausted because the growth rate is very fast. When the D.O. rises sharply, due to the depletion

of octane, 50 ml octane is added, and this process is repeated as often as necessary (~2 hrs. intervals) to obtain the desired D.O. of the cells at chart zero. Usually 4-5 additions of octane are needed before harvest at late log phase (~16 hrs.) as shown in a typical growth curve (Figure 3). Since the pH of the growing medium tends to be lowered by metabolites, it was periodically adjusted by the addition of 5N NaOH. The cells were collected by centrifugation at 10,000xg for 5 min. and the pellets were stored at -20°. Typically, 400 g (wet weight) of highly active cells, determined by epoxide assay (see below), were obtained from each 10 l fermentation.

Resting Cell Assay for Epoxide Formation (53-55)

Two ml of the cell suspension from a master flask was added to a small shake flask containing 100 ml of P-1 medium. Following growth, the cell suspension was washed twice by centrifugation (10,000 xg, 10 min.), with 100 ml 0.1 M phosphate buffer pH 7, containing two drops of Triton X-100. The final cell pellet was suspended in buffer to yield an $\text{O.D.}_{660} = 18$, which is equivalent to a viable titer of $2 \times 10^9/\text{ml}$. To a small shake flask was added 10 ml of this cell suspension and 0.1 ml octadiene. After incubation at 30° in the shaker, 1 ml samples were removed at each 1 hr. period and extracted with 0.5 ml hexane containing 2-octanol (10 $\mu\text{l}/\text{ml}$) as internal standard. The emulsion formed was broken by centrifugation (5,000 x g, 3 min.) at room temperature, and the upper hexane layer was analyzed for 7,8-epoxy-1-octene by flame

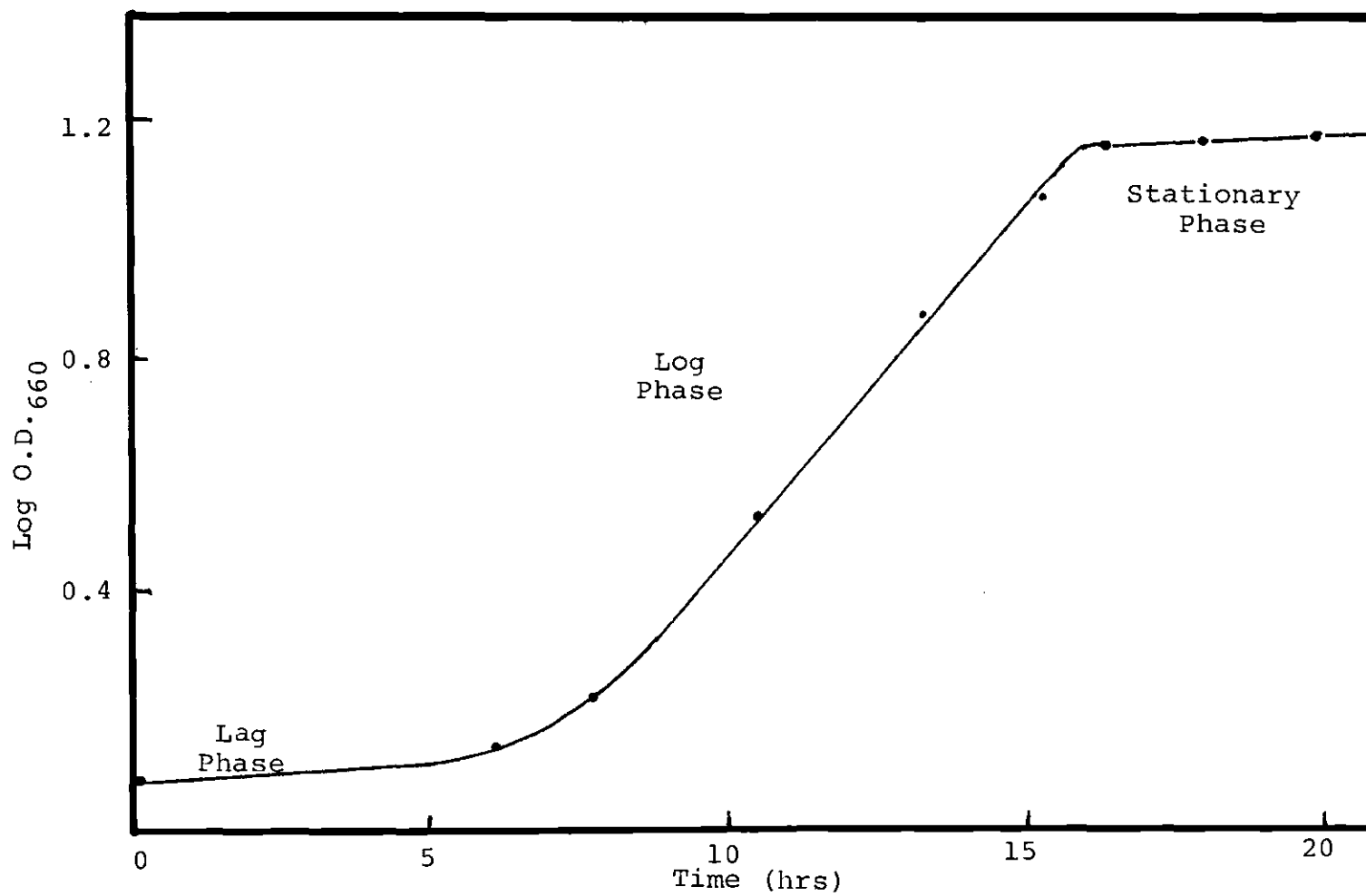


Figure 3. Growth Curve of *P. oleovorans* in the Fermentor.

ionization gas chromatography (Varian) using a 20 ft. x 1/8 in. column of 10% carbowax 20 M on 80/100 chromosorb W maintained isothermally at 180°.

Assay of Rubredoxin by Cytochrome c Reduction

Varying amounts of soluble (Co- or Fe-) rubredoxin or rubredoxin conjugates were added to cytochrome c in 0.05 M Tris-Cl at pH 7.8, and the mixtures incubated at 30° for 3 min. Aliquots of NADH (or NADPH) and rubredoxin-reductase (or spinach reductase) were then added to initiate the reaction. Cytochrome c reduction was monitored at 550 nm using $\Delta\epsilon_M = 21,000 \text{ M}^{-1}\text{cm}^{-1}$ (56). Background activity due to the presence of the cofactor and reductase was corrected. The ACTA spectrophotometer used in these experiments was equipped with a built-in magnetic stirring system, which was essential for kinetic experiments with rubredoxin-Sepharose conjugates.

Assay Based on Reduction of the Rubredoxin Chromophore

The conditions were similar to those described above for the measurement of cytochrome c reduction except that the cytochrome c was omitted, and the amount of rubredoxin was increased. The rate of rubredoxin reduction, measured by the decrease in absorbance at 497 nm was then determined. Since the rate of rubredoxin reduction was found to be linear with respect to the reductase concentration, the reductase activity was determined by a similar assay using varying amounts of reductase and monitoring the decrease at A_{497} .

Protein Determinations

Protein concentrations were estimated by the Bio-Rad assay method (57) throughout the purification of the rubredoxin. Aliquots of protein solution were diluted to 100 μ l with 0.05 M KH_2PO_4 buffer containing 0.15 M NaCl at pH 7.3, followed by the addition of 5 ml dye, according to the manufacturers' instructions. The amount of protein was then calculated from the absorbance (vs. dye blank) at 595 nm. The standard curve was made by using known concentrations of bovine γ -globulin.

For spectrophotometric determinations of rubredoxin concentrations, the following ϵ_M values were used (11):

$\epsilon_{M_{280 \text{ nm}}} = 37,700 \text{ M}^{-1}\text{cm}^{-1}$ for (1Fe)-rubredoxin, $\epsilon_{M_{280 \text{ nm}}} = 39,500 \text{ M}^{-1}\text{cm}^{-1}$ for (2Fe)-rubredoxin, and $\epsilon_{M_{277 \text{ nm}}} = 34,013 \text{ M}^{-1}\text{cm}^{-1}$ for aporubredoxin.

Isolation of Rubredoxin

The general procedure used was similar to that of Lode and Coon (11) with some modifications. Unless otherwise stated, all operations were performed at 4° in Tris-Cl buffer pH 7.3., and the centrifugations was at 20,000 xg. The A_{280}/A_{497} ratios were routinely used as an index of purity. The protein peaks from each chromatography were detected by an ISCO Model UA-5 absorbance monitor at 280 nm with a light path of 0.1 cm and the scale of 2.0. The flow rate of the elution was controlled either by an ISCO Model 312 metering pump or a Buchler peristaltic pump. Fractions were collected

in an ISCO Model 328 fraction collector.

Frozen cells (1 kg) were allowed to thaw overnight at 4°. The cell paste was mixed with 1.1 % of 0.01 M Tris base and homogenized for 1 min. with a blender at medium speed. After adjusting pH to 7.6 with 1 M Tris base, about 5 mg each of DNase and RNase, followed by 0.5 ml 2-mercaptoethanol were added to the cell suspension. The cells were sonically disrupted for 4 min. in bursts of ~1 min. followed by cooling for 1 min. in 250 ml portions using an Artek #300 Sonic Dismembrator at full output, and the temperature was kept below 11° by the use of an ice-salt bath. The sonically disrupted mixture was stirred with streptomycin sulfate (10 g/200 ml water) for 30 min., then centrifuged again for 50 min. Solid ammonium sulfate was slowly added over at least 3 hrs. to the supernatant (170 g/l) give 30% saturation at pH 7.4, 4° and centrifuged for 20 min. The resultant precipitate was resuspended in 0.02 M Tris-Cl pH 7.3 and transferred to several dialysis bags, which had been treated by heating in two washes of 50% EtOH-H₂O followed by two washes with 10 mM NaHCO₃, then 1 mM EDTA (1 hr. each), and deionized water, sequentially and all at room temperature. The bags containing 30-60% ammonium sulfate precipitate were placed in an ISCO automatic dialyzer (ISCO Model 390) through which 20 liters of 0.02 Tris-Cl was passed. The deep brown solution was collected and applied to a column (5.2 x 40 cm) of Whatman DE-52, which had been carefully packed and equilibrated with 0.1 M buffer.

Elution was started by 0.02 M buffer, which eluted all pink, neutral to alkaline-insoluble material. The column was then washed with 0.1 M buffer followed by 0.1 M KCl in 0.1 M buffer. At this point, the rubredoxin, which could be seen as a red-brown band half way down the column was eluted by means of a KCl gradient produced by siphoning 1.0 liter of 0.5 M KCl in 0.1 M buffer into an equal volume of 0.1 M KCl in the same buffer (Figure 4 and Table 2). The rubredoxin was eluted from the column at about 0.2 M KCl and fractions with A_{280}/A_{497} ratio smaller than 19 typically about 170 ml were pooled and concentrated by ultrafiltration with a UM-10 membrane in an Amicon cell to less than 20 ml. The concentrated rubredoxin was then applied to a 2.6 x 77 cm column of Sephadex G-75 which had been equilibrated with 0.1 M buffer (Figure 5). Fractions containing rubredoxin with A_{280}/A_{497} ratio smaller than 14 were pooled and applied to second DE-52 cellulose column (2.6 x 26 cm), preequilibrated with 0.1 M buffer. Elution was accomplished with a 0.1 M to 0.5 M Tris-Cl gradient, 300 ml each, and the rubredoxin eluted from the column at about 0.35 M buffer (Figure 6). The fractions containing rubredoxin were concentrated, and then applied to second Sephadex G-75 column (2.6 x 77 cm), preequilibrated with 0.1 M buffer (Figure 7). The rubredoxin fraction at this stage is very pure with A_{280}/A_{497} ratio smaller than 7. A summary of a typical preparation is outlined in Table 3. As reported by Lode and Coon, we observed that the $A_{280}:A_{497}$ ratio of

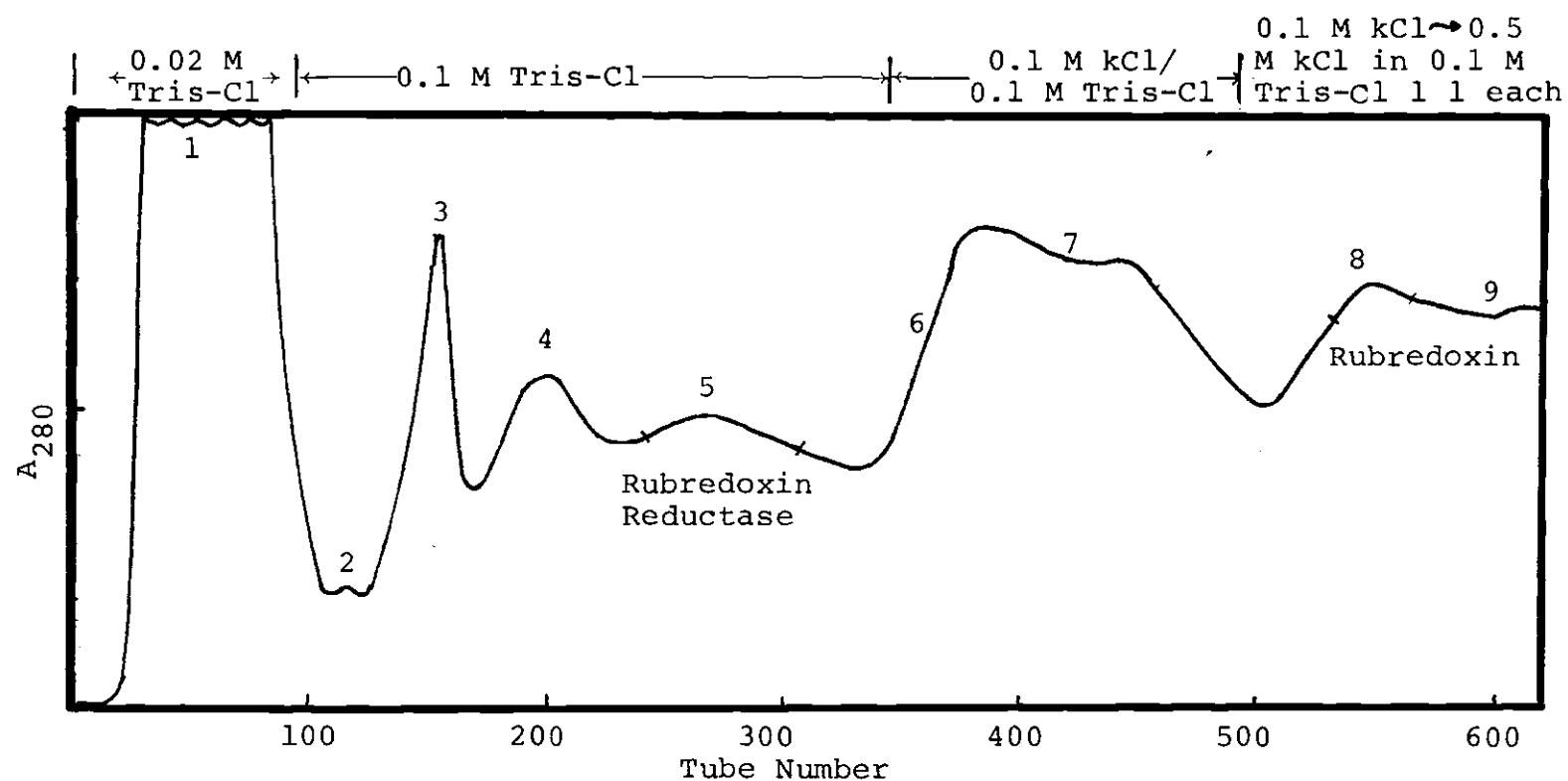


Figure 4. DEAE Chromatography of 30-60% Ammonium Sulfate Fractionation From Sonicate Extract. Column: 5.2 x 40 cm, equilibrated with 0.1 M buffer; flow rate: 12ml/7 min/tube; sample applied: 425 ml crude solution in 0.02 M Tris-Cl; all solutions were at pH 7.3.

Table 2. Characteristics of Fractions From First DEAE Chromatography.

<u>Fraction</u>	<u>Elution Condition</u>	<u>Color</u>	<u>λ_{max} (nm)</u>	<u>Activity</u>
1.	0.02 M Tris-Cl	insoluble pink	-	Yes ^a
2.	0.02 M Tris-Cl	green yellow	380,450	No ^b
3.	0.1 M Tris-Cl	turbid yellow	410	No ^b
4.	0.1 M Tris-Cl	pale yellow	360,410,438	No ^{b,d}
5.	0.1 M Tris-Cl	pale yellow	360,438	Yes ^{a,b,c}
6.	0.1 M KCl/0.1 M Tris-Cl	turbid white	410	No ^a
7.	0.1 M KCl/0.1 M Tris-Cl	bright yellow	410	No ^a
8.	0.2 M KCl/0.1 M Tris-Cl	red-brown	380,497	Yes ^{a,c}
9.	0.4 M KCl/0.1 M Tris-Cl	bright yellow	360,450	No ^b

a. G.C. assay for epoxide formation.

b. Reduction of Rubredoxin (A_{497}) in the presence of NADH.

c. Cytochrome c assay.

d. This fraction is a mixture of fraction 3 and fraction 5, and the activity is much less than that of the latter.

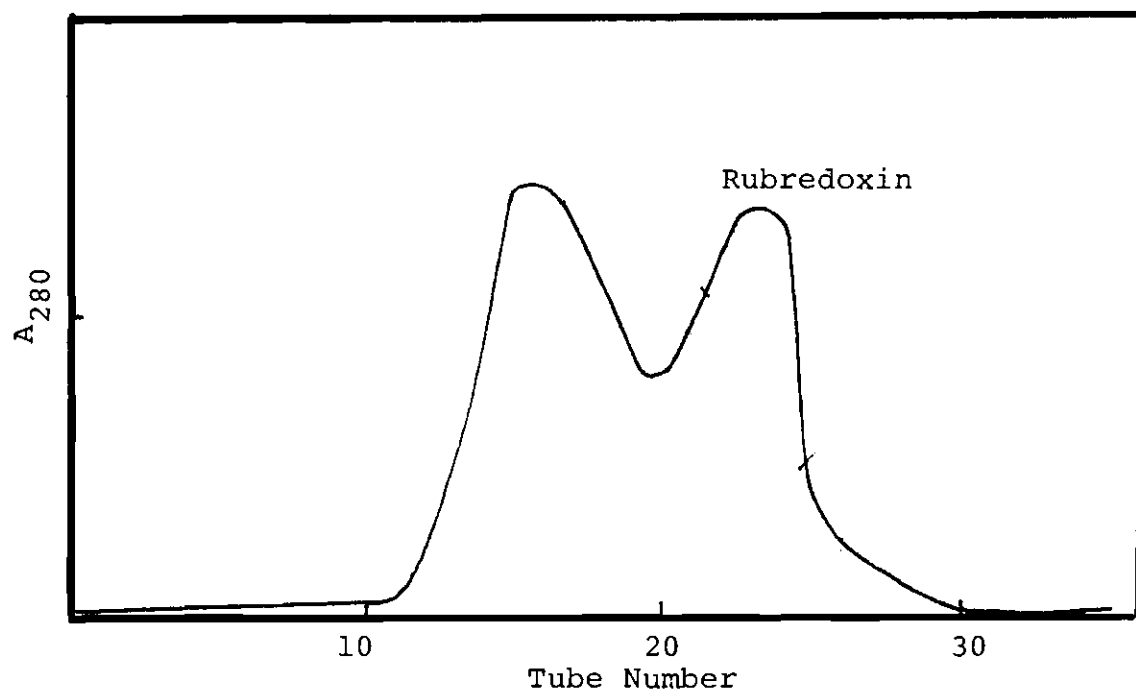


Figure 5. Sephadex G-75 Chromatography of Rubredoxin concentrate from DEAE Elution. Column: 2.6 x 77 cm; elution buffer: 0.1 M Tris-Cl, pH 7.3; flow rate: 8 ml/6 min/tube; sample applied: fraction 8 from DEAE, 10 ml concentrate in 0.2 M Tris-Cl.

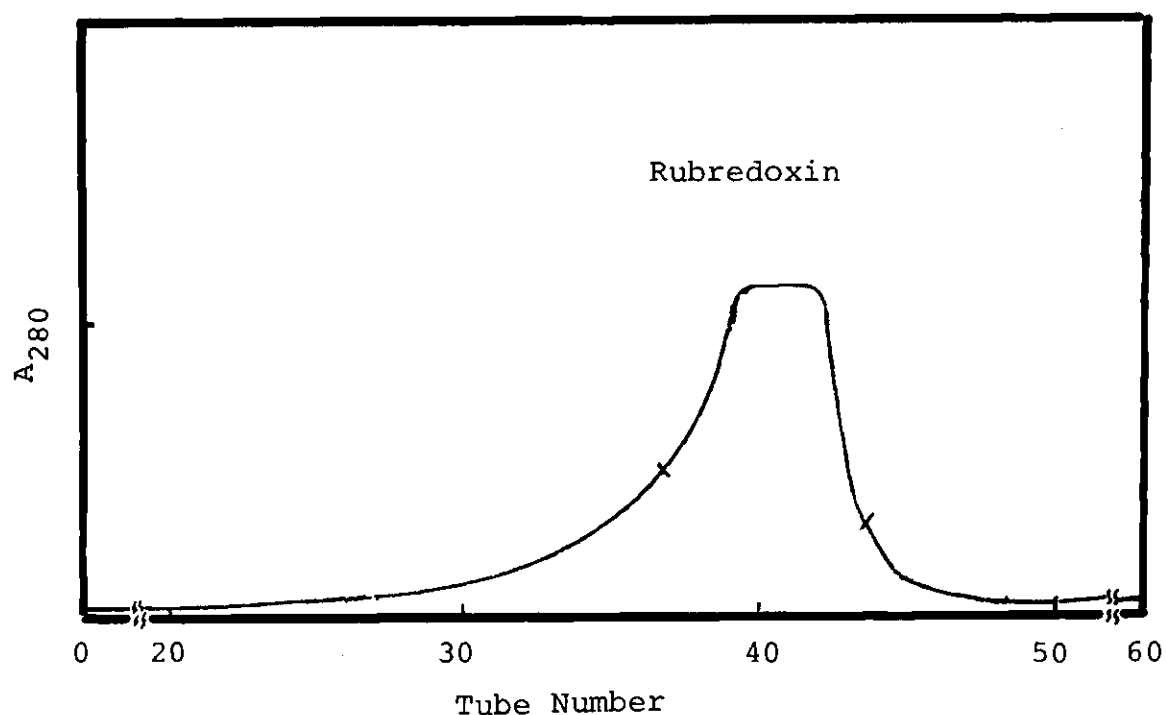


Figure 6. Second DEAE Chromatography of Rubredoxin From Sephadex G-75 Elution. Column: 2.6 x 26 cm; elution buffer: 0.1 M Tris-Cl to 0.5 M Tris-Cl gradient, 300 ml each, pH 7.3; flow rate: 10 ml/6 min/tube; sample applied: the 2nd fraction from G-75, 75 ml total in 0.1 M Tris-Cl.

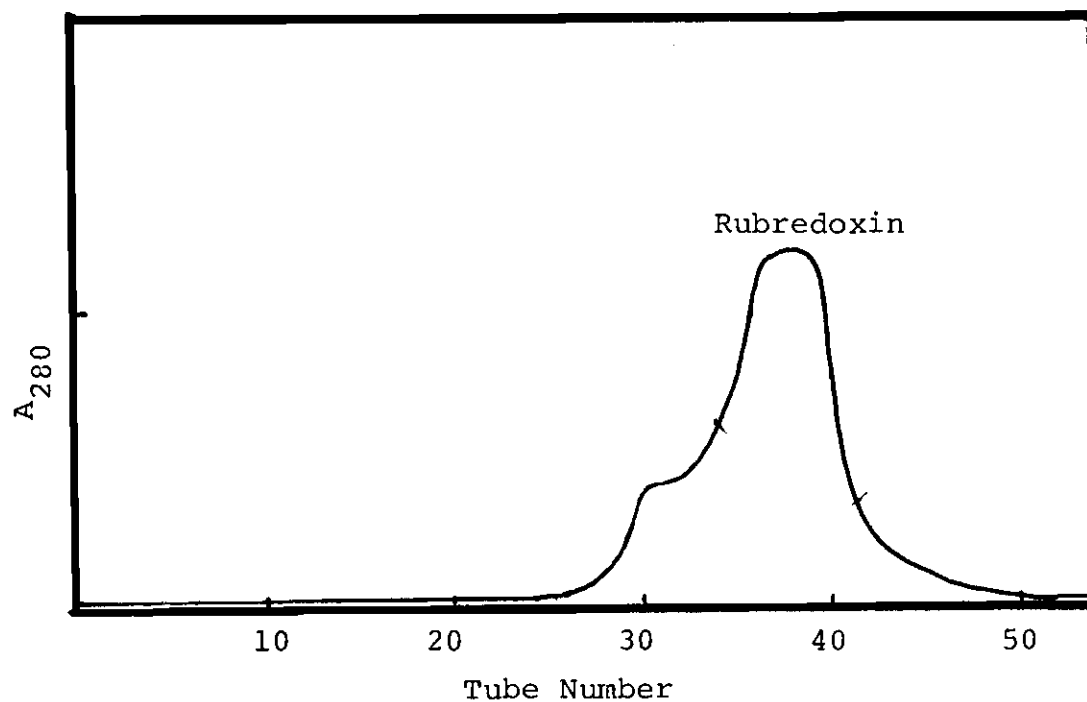


Figure 7. Second Sephadex G-75 Chromatography of Rubredoxin From Second DEAE Elution. Column: 2.6 x 77 cm; elution buffer: 0.1 M Tris-Cl, pH 7.3; flow rate: 5 ml/6 min/tube; sample applied: fraction from second DEAE, 10 ml concentrate in 0.35 M Tris-Cl.

Table 3. Preparation of Rubredoxin From 1 kg Cells.

Step	Protein ^a (g)	Volume (ml)	A_{280}/A_{497} ^b	A_{380}/A_{497} ^b
1. Sonicate extract	96.0	2000	-	-
2. Streptomycin supernatant solution	60.0	1950	-	-
3. Ammonium sulfate precipitation (30-60% saturation)	26.9	420	-	-
4. First DE-52 column eluate	0.500	170	18.5	1.53
5. First G-75 column eluate	0.322	75	14.1	1.47
6. Second DE-52 column eluate	0.151	42	10.0	1.20
7. Second G-75 column eluate	0.133	65	6.8	1.12

a. Bio-Rad protein assay.

b. Spectral data is for pooled fractions after each step.

the stored material increases upon storage, indicating gradual release of the iron from the chromophores (11).

Isolation of Spinach Ferredoxin - NADP Reductase

The procedure was similar to the method of Shin (58). 1 kg of fresh, unfrozen spinach leaves, previously deveined and washed with water, were ground for 2 min. in 1 liter of ice water in a Waring Blender. The deep green homogenate was filtered through a double layer of cheesecloth on a large Buchner funnel to remove debris. The filtrate (~3 l) was adjusted to pH 7.6 with 1 M Tris base (~17 ml), followed by the addition of 1.5 liters of acetone at -15° to 35% (V/V). The supernatant collected after centrifugation (5,000 x g, 10 min.) was further treated with cold acetone to a final concentration of 75% (V/V). The deep brown precipitate was collected by centrifugation at 3,000 x g for 10 min. at 4°, then washed twice with cold acetone. The residual acetone was vaporized in air by spreading the precipitate over large filter paper at 4°. The particles were dissolved in 350 ml of 0.06 M Tris-Cl at pH 7.3 and centrifuged to remove insoluble material, then applied to a DE-52 column (4.2 x 25 cm), pre-equilibrated at a 0.1 M Tris-Cl at the same pH and washed with the same buffer (Figure 8). The yellow band of enzyme, which does not adsorb to the cellulose in this buffer, was collected and fractionated with ammonium sulfate, in the presence of 50 mM Na-pyrophosphate at pH 7.8. The 40-65% ammonium sulfate precipitate was dissolved in 0.04 M Tris-Cl

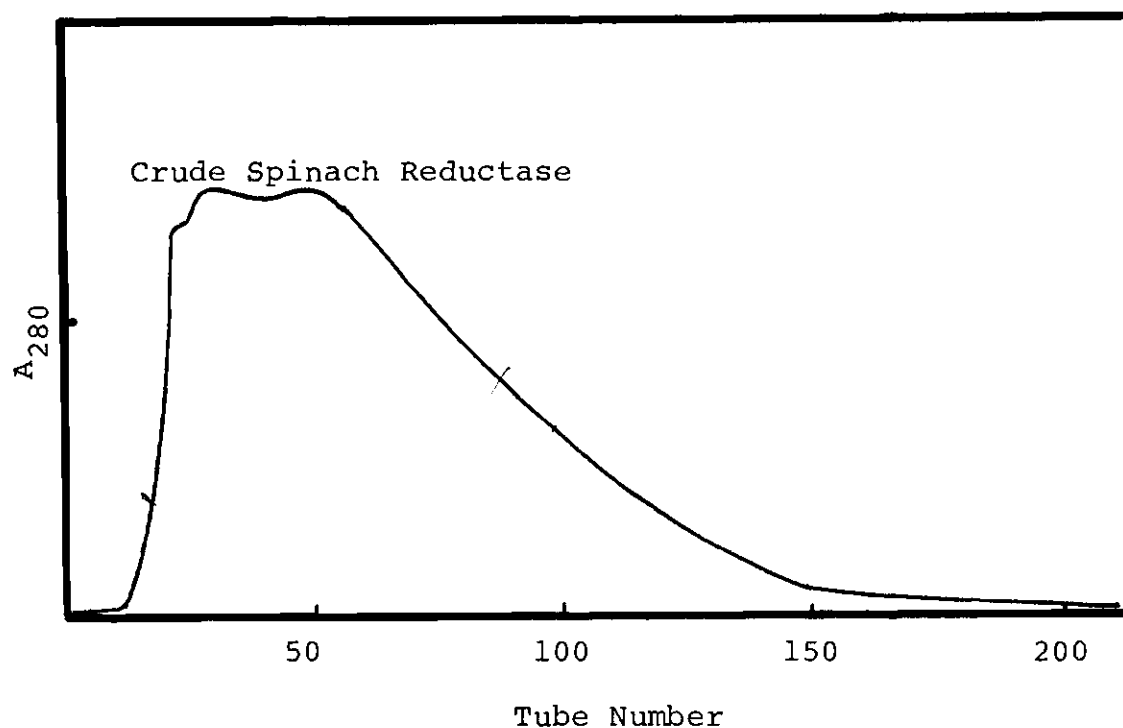


Figure 8. DEAE Chromatography of 35-75% Acetone Fractionation From Spinach Homogenates. Column: 4.2 x 25 cm, equilibrated with elution buffer; elution buffer: 0.75 M Tris-Cl, pH 7.3; flow rate: 8 ml/3 min/tube; sample applied: 300 ml in 0.058 M Tris-Cl.

at pH 7.9 and passed through a Sephadex G-50 column (2.6 x 90 cm), preequilibrated with the same buffer (Figure 9). The first fraction was diluted three times with water and applied to DE-52 column (4.2 x 15 cm), preequilibrated with 0.04 M Tris-Cl (Figure 10). The pure reductase ($A_{456}:A_{475} = 0.1$) was eluted at 0.3 M Tris-Cl. Typical yield is 20 mg, calculated from $\epsilon_M = 10,740$ at 456 nm (57).

Preparation of Alkyl and ω -Aminoalkyl Sepharose

CNBr-activated Sepharose for the coupling was obtained either from Pharmacia or by the following preparation (59, 60):

About 30 g of well washed, decanted Sepharose was mixed with 30 ml of water and 60 ml of 2 M Na_2CO_3 by stirring slowly at 4°. The rate of stirring was increased and 5 ml of an acetonitrile solution containing 5 g CNBr was added immediately at once. The slurry was stirred vigorously for 5 min., after which the slurry, was filtered and washed as described by March (60).

The ligands to be coupled, 20 mmoles each of n-octylamine, 1,6-diaminohexane or 1,8-diaminooctane in 10 ml each of 0.1 M NaHCO_3 buffer at pH 10 were then added to an equal volume of packed Sepharose, individually in three polyethylene tubes. Each suspension was immediately mixed end over end for 16 hrs. at 4°. Each substituted Sepharose was then washed with large volumes of 0.5 M NaCl, water, and finally with 5 mM sodium phosphate buffer at pH 7.3.

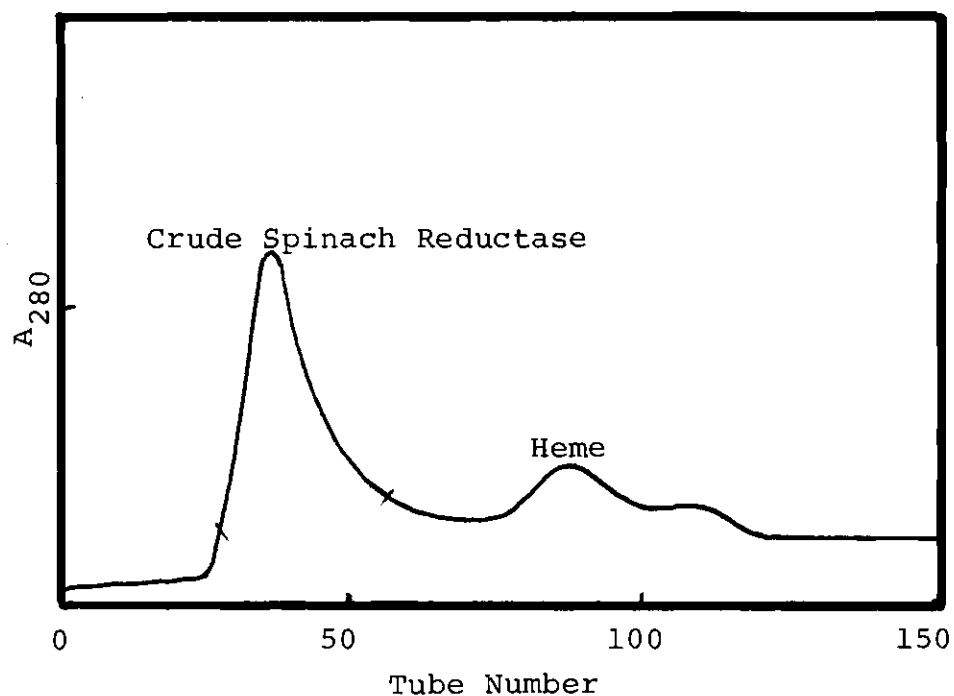


Figure 9. Sephadex G-50 Chromatography of 40-65% Ammonium Sulfate Fractionation From DEAE Elution. Column: 2.6 x 90 cm, equilibrated with elution buffer; elution buffer: 0.137 M Tris-Cl; flow rate: 6 ml/3 min/tube; sample applied: 10 ml in elution buffer.

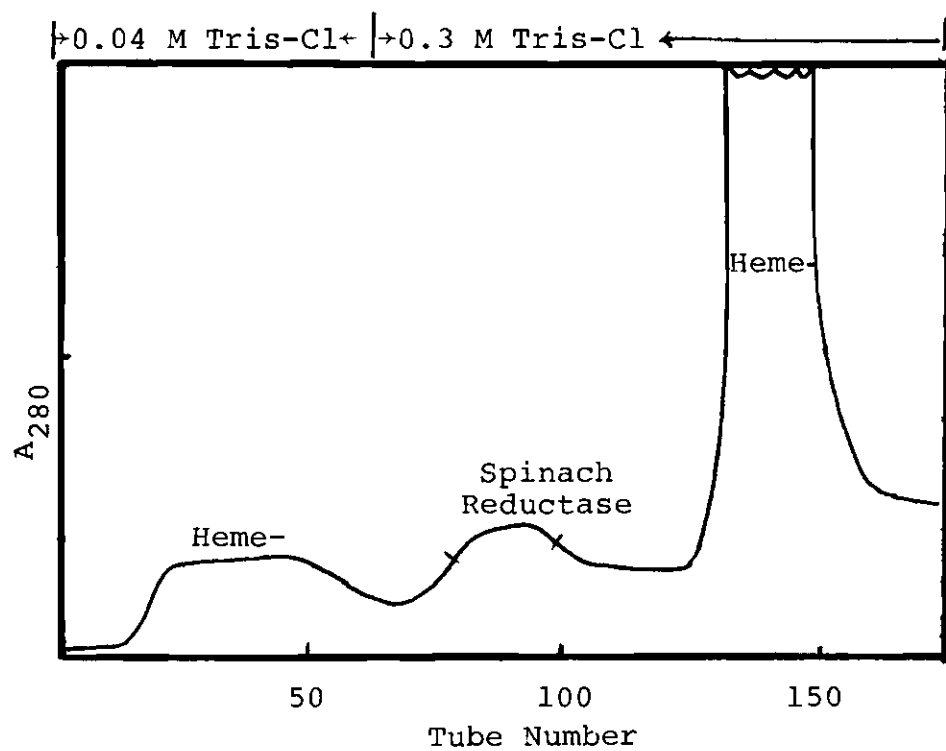


Figure 10. DEAE Chromatography of Yellow Eluate From Sephadex G-50 Chromatography.
Column: 4.2 x 15 cm

For color test (61), a small quantity of the derivatized gel (0.5 ml) was added to a solution of sodium borate (saturated, 1 ml) and three drops of a 3% aqueous solution of sodium 2,4,6-trinitrobenzene sulphonate (TNBS) added. The color was allowed to develop for 2 hrs. at room temperature. The Sepharose derivatives containing primary aliphatic amines formed orange products.

Isolation of Rubredoxin Reductase

Fraction 5 from the first DEAE chromatography (Figure 4) was essentially a fraction containing crude reductase (Table 2) after dialysis against 5 mM phosphate buffer at pH 7.3, aliquots of the proteins were chromatographed on either immobilized rubredoxin (see below) or one of the Sepharose derivatives described above. For large scale purification, a 45-70% fractionation of fraction 4 by solid ammonium sulfate was first carried out at 4°. The precipitate was then dialyzed against 5 mM phosphate buffer at pH 7.3, or pooled on a Bio-gel A (0.5 m) column equilibrated with the same buffer before applying to the affinity column.

For the purpose of this purification, 4 g of CNBr-activated Sepharose for rubredoxin immobilization was prepared using 125 mg CNBr in 10 ml cold water by March's method (60). The activation proceeded for 5 min. at 4°. Coupling of rubredoxin was then carried out in 0.1 M NaHCO_3 , pH 8.0 at 4° for 15 hrs.

The reductase bound, if any, in the column was eluated

at the increasing concentration of phosphate buffer produced by the technique of gradient elution. The purity of the reductase was judged by A_{272}/A_{438} ratio. The reductase was stored in 25 mM phosphate buffer containing 10% glycerol at -20° .

Disc Gel Electrophoresis

The experiment was carried out as described by Davis (62) with large pore stacking gel (7%) solution at pH 8.8, small pore separating gel (7%) solution at pH 9.5, and Tris-glycin buffer at pH 8.8 in the presence of 5 mA/tube for 1 hr. The gels were stained with Coomassie Blue (0.05%) and desalted with 7% acetic acid.

Isoelectrofocusing

The electrofocusing column was set up according to the instruction manual (LKB), with the cathode at the top and the anode at the bottom of the column. The cathode bath was 10 ml of a dilute aqueous solution of NaOH (1%, W/V). The anode bath was 20 ml of a phosphoric acid (1%, V/V) and sugar (60%, W/V) solution. Dense solution was prepared from 2.25 ml ampholine (pH range 3.0 to 10.0 or 3.5 to 5.0) plus 28 g sucrose in deionized water to a final volume of 60 ml. Light solution was prepared by dissolving 0.75 ml of the same ampholine in 60 ml deionized water. The density gradient was produced by mixing proper amounts of Dense and Light solution using two burettes, and was then carefully pumped into the compartment in the direction of dense to light. The

proper amount of protein (5-10 mg) solution was included in place of light in the middle of the compartment. The compartment was then subjected to 500 v, occasionally increased to maintain a current of 9 mA for 24 hrs. The solution in compartment was then passed through an absorbance monitor (at 280 nm) to a fraction collector (2 ml/fraction). The pH of protein effluent was measured at 4°. Runs were also performed with ampholine up to 5%, or in the presence of 5% sulfobetaine DLH or 1% Triton X-100. Despite these various attempts to solubilize or "salt in" the protein, severe precipitation of rubredoxin at its isoelectric point always occurred.

Preparation of Immobilized Rubredoxin

Activation of Sepharose 4B with CNBr was carried out following the procedure of March, et al. (60). This procedure employs a high concentration of sodium carbonate for pH control, and the CNBr is added as a solution in acetonitrile (2 g/ml). After CNBr addition, the slurry of Sepharose was stirred for 2 min., filtered, and washed as described by March. Prior to coupling step, the rubredoxin was concentrated, carefully dialyzed against 0.2 M sodium bicarbonate, pH 9.5, to remove Tris buffer, and then coupled immediately to the freshly activated gel. Coupling was carried out in pH 9.5 bicarbonate buffer at 4° for 20 hrs., after which unreacted rubredoxin was removed by vacuum filtration, and the gel washed with a small amount of coupling buffer. Five ml of 1 M ethanolamine were added and stirring was continued for 2 hrs. at pH 9.0

and 25° in order to block any remaining active groups on the gel. After coupling, the beads were washed alternately with at least 25 volumes each of 0.1 M sodium acetate (pH 4) and 0.1 M sodium bicarbonate (pH 10), each of which also contained 0.5 M NaCl. Finally the beads were washed with deionized water to neutrality and then exhaustively with 0.1 M Tris-Cl, at pH 7.3. Typically, about 25 mg of rubredoxin and 20 ml of the 1:1 Sepharose/water slurry were used in the coupling reaction. The immobilized enzyme preparations were stored at 4° in pH 7.3 Tris buffer. Upon storage, we observed a loss of about 5% per month in the A_{497} , presumably reflecting slow leaching of iron from the protein.

Amino Acid Analysis

Acid hydrolyses with 6 N HCl at 110° were carried in vacuo for 22 hrs., prior to the analyses, and norleucine was used as the internal standard. In the case of immobilized rubredoxin, the gels, which had been washed extensively after coupling, were washed successively with water, then water/acetone mixtures of increasing acetone concentration, and finally with pure acetone. The shrunken gels were then dried over phosphorus pentoxide in vacuo at 100° for 20 hrs. Weighted amounts of conjugates (and of CNBr-activated Sepharose as a control) were hydrolyzed and analyzed in the same fashion as the soluble enzyme. The standard amino acid mixture (0.1000 μ mole each) including norleucine (0.1005 μ mole) was run first. The concentration of each amino acid in the protein was then

calculated as follows:

- (1) Calculate the peak area (width x half height x 2400, where 2400 is a color factor) for each amino acid with correction for baseline drift, if necessary.
- (2) Divide the μ moles of each amino acid in the standard by its peak area.
- (3) Multiply the corrected peak area of each amino acid in the protein by the corresponding value obtained from (2).
- (4) Calculate % recovery for norleucine, i.e.,
$$\frac{\text{Norleucine found}}{\text{Norleucine applied}} \times 100$$
- (5) Correct each value of amino acid content from (3) by the % recovery obtained in (4).
- (6) Subtract the values contributed by the CNBr-Sepharose blank obtained as above (1)-(5).
- (7) Calculate numbers of residues for each amino acid in the protein, based on isoleucine (6 residues/mole rubredoxin).

For immobilized rubredoxin, the protein content of the gels (mg/g of dry support) was calculated from the recovery of aspartic and glutamic acid. No complications from the high carbohydrate contents of the samples were encountered; similar observations have been reported by other investigators (63-65). A typical amino acid analysis of the rubredoxin conjugate is shown in Table 4.

Table 4. Data of Amino Acid Analysis

Amino Acid	Standard ^a (0.1000 μmole of each)	Control ^{a,b,c}	10 X μmole	Conjugate ^{a,c}	10 X μmole	10 X μmole (Net)	Moles ^d /Per Mole Protein
Lysine	1819	0	-	2178	1.205	1.205	6.6
Histidine	1632	0	-	1094	0.870	0.870	4.8
Ammonia	1344	2158	1.733	2207	1.650	-	-
Arginine	1642	0	-	1714	1.050	1.05	5.8
Met-O	626	887	1.520	-	-	-	-
Aspartic acid	1564	51	0.034	5624	3.617	3.583	19.7
Threonine	1548	32	0.021	2931	1.904	1.883	10.3
Serine	1515	118	0.084	2797	1.857	1.773	9.7
Glutamic acid	1613	71	0.047	5721	3.568	3.521	19.3
Proline	53	3	0.060	127	2.410	2.350	13.0
Glycine	1546	194	0.135	4694	3.054	2.919	16.0
Alanine	1636	61	0.040	4449	2.735	2.695	14.8
Half-cystine	865	295	0.367	528	0.613	0.246	1.4
Valine	1737	0	0	3428	1.985	1.985	10.9
Methionine	1575	0	0	412	0.263	0.263	1.4
Isoleucine	1637	48	0.031	1829	1.123	1.092	6.0
Leucine	1585	54	0.037	3920	2.487	2.450	13.4
Tyrosine	1544	28	0.019	1210	0.788	0.769	4.2
Phenylalanine	1547	29	0.020	1430	0.930	0.910	4.9
Norleucine	1571	828	0.568	888	0.569	-	-

a. The values are peak area after correction from the chart.

b. Same weight of CNBr-activated Sepharose 4B as that of the conjugate.

c. Samples were applied with 0.0569 μmole of Norleucine as internal standard.

d. Assuming 0.1092 μmole equivalent to 6 moles of isoleucine/mole protein.

Spectrophotometric Measurement of Immobilized Rubredoxin

The measurements were carried out using ACTA MVI spectrophotometer equipped with a scattered transmission accessory. This accessory obviated the necessity for dilution of the immobilized enzyme before absorption spectral measurements. In all cases, the gel was gravity-packed in a 10 mm path length semimicrocuvette for several hours. To demonstrate that this settling procedure always gives packed gel of constant density individual test tubes containing gravity-packed gel of different volumes were dried in vacuo at either 60° or 110° to constant weight, and from these experiments it was found that 1 ml of gravity-packed gel is reproducible equivalent to 27 mg dry weight. This value differs considerably from that reported by Koelsch, et al. with Sepharose 6 B (66). Spectra of immobilized enzyme were obtained using either Sepharose or CNBr-activated Sepharose 4 B in the reference cuvette. In the former case, the spectra were displaced toward high absorbance by an amount which uniformly corresponded to the difference spectra between CNBr-activated Sepharose and Sepharose.

Anaerobic Reduction of Immobilized Rubredoxin

In a dry box, solid Na-dithionite was added to nitrogen-saturated 0.1 M pyrophosphate buffer at pH 8.3, to give a solution of the desired concentration. A Thunberg cell containing immobilized rubredoxin was then purged with nitrogen for 1 hr. after which it was transferred to the dry box.

The cell was opened, a slight excess of dithionite was added, mixed with the conjugate, and then allowed to completely re-settle before the spectrum of the reduced enzyme was recorded. Enzymatic reduction was accomplished by adding 0.05 mg of spinach reductase and a slight excess of NADPH to the Thunberg cell in the place of dithionite.

Reduction Potential Measurement of Immobilized Rubredoxin

A reaction mixture containing 2.4 ml gravity-packed conjugate and 40 n mole of indigo carmine ($\lambda_{\text{max}} = 613 \text{ nm}$, $\epsilon_M = 2.22 \times 10^4$) (67) in 0.1 M Tris-Cl at pH 7.0 in a specially constructed anaerobic cell was alternatively evacuated and flushed with purified nitrogen at least three times. The spectra were recorded on settled gel alone, settled gel plus dye after mixing and resettling, and the complete system after addition of 120 nmole of NADPH plus 4 nmole of spinach reductase followed by mixing and resettling. Settling was always carried out with the cell in a dry box under a nitrogen atmosphere. The reference cell contained CNBr-activated Sepharose. The specially constructed anaerobic cell allows facile alternate evacuation and efficient nitrogen flushing. This anaerobic cell was so constructed as to allow the contents to be magnetically stirred with the ACTA stirring sphere when desired, a feature which was essential in experiments with the immobilized conjugate. The following form of Nernst equation was used to calculate $E_{m,7}$ for the conjugate.

$$E_{m,7} \text{ conj} + \frac{RT}{nF} \ln \frac{\text{oxidized conj}}{\text{reduced conj}}$$

$$= E_{m,7} \text{ dye} + \frac{RT}{nF} \ln \frac{\text{oxidized dye}}{\text{reduced dye}}$$

where R is gas constant; T, the absolute temp.; F is the faraday; and $\frac{RT}{F} = 0.059$ at 25°

n = 1 for the conjugate assuming 1 electron
was accepted during enzymatic reaction
(i.e., only 1 Fe/mole conjugate)

n = 2 for Indigo carmine (67)

$E_{m,7} \text{ dye} = -0.116 \text{ v}$ at pH 7.0 and 25° (68).

The percent reduction of both the conjugate and Indigo carmine was determined from the difference spectrum, partially reduced minus fully oxidized system at equilibrium, to calculate a redox potential of $E_{m,7}$ conjugate according to Nernst equation described above.

Reconstitution of Immobilized Rubredoxin

Iron lability from rubredoxin was increased upon reduction to the ferrous state. Accordingly, immobilized rubredoxin was conveniently converted to the apoenzyme by anaerobic reduction in the presence of excess dithionite, after which it was extensively washed with 0.5 M tris base containing 0.07 M mercaptoethanol to give a colorless conjugate. The washed apoenzyme conjugate was then purged with nitrogen for 2 hrs. at room temperature followed by the addition of 100 μ l 0.1 M ferrous ammonium sulfate to give a yellow-red suspension. After purging for an additional 10 min. with stirring, air

was admitted, turning the conjugate dark red. After successive washing with water, coupling buffer (pH 9.5, 0.5 M NaCl), acetate buffer (pH 4.0, 0.5 M NaCl), and 0.1 M Tris-Cl, pH 7.3, containing 0.1 M KCl, the gel was gravity-packed and examined spectrophotometrically.

Stability Comparison of Soluble and Immobilized Rubredoxin

In separate experiments, soluble rubredoxin (0.3 mg/ml), washed Sepharose 4B which had been suspended in the presence of 0.3 mg/ml rubredoxin and then gravity packed (settled volume 1.2 ml), and rubredoxin-Sepharose conjugate (1.2 ml settled volume, $A_{497} = 0.32$) were mixed with concentrated guanidine HCl to give a guanidine HCl concentration of 2.5 M and then incubated at 30°. At the time periods, absorbance measurements were taken on the samples.

Preparation of Aporubredoxin

Rubredoxin was precipitated by trichloroacetic acid in the presence of 0.5 M mercaptoethanol under nitrogen. The precipitate was resuspended in 10% acetic acid in a dialysis bag, and was further dialyzed against 60 volumes of the same solution at 4° for at least 24 hrs. with several changes of fresh acid. The protein precipitate slowly went back into solution during dialysis. After lyophilization, the material was stored at -20°. The apoenzyme thus obtained exhibited no visible absorbance indicating loss of the iron chromophore. As a further test for complete iron removal, assay of residual electron transfer activity was carried out using cytochrome c

in the presence of rubredoxin reductase and NADH. The iron content of aporubredoxin was further examined by atomic absorption spectrometry to confirm complete iron removal.

Preparation of Reconstituted Rubredoxin

The methods used to prepare (2Fe)- and (2Co)-rubredoxin were derived from methods previously described by Lode and Coon (11). The new method is somewhat simpler and avoids the possible metal contamination from repeated precipitation by trichloroacetic acid, which usually results in insoluble protein in reconstitution mixtures. The lyophilized apoprotein was dissolved at a final concentration of 5 mg per ml in a 0.5 M Tris base containing 0.06 M mercaptoethanol and the clear colorless solution was flushed with nitrogen for 5 min. After incubation at room temperature under nitrogen for 3 hrs., a freshly prepared aqueous solution of spectrographically pure cobalt sulfate or cobalt chloride was added. The molar concentration was twice that of aporubredoxin. The green-colored mixture was allowed to stand under nitrogen for 10 min., after which it was readily oxidized by exposure to the air to give a light yellow product [c.f. similar observation with the cobalt (II) complexes of Boc-(Gly-L-Cys-Gly)₄-NH₂ (49)]. G-25 Sephadex, preequilibrated with 0.05 M Tris-Cl at pH 7.3 was used for desalting at 4°. Two iron rubredoxin was also prepared by the same procedure but with ferrous ammonium sulfate as the iron source. The reconstitution mixtures were pink and deep red, respectively before and after exposure

to the air. A two fold molar excess of either salt with respect to the apoprotein was added to reconstituting mixtures in all cases. A comparative ligation study was also performed with various stoichiometric amounts of both iron and cobalt salts. The iron and cobalt content was measured by atomic absorption (Perkin Elmer, Model 460) at 248.3 and 240.7 nm, respectively. Concentrations of either cobalt or iron rubredoxin or mixtures, were determined spectrophotometrically at 280 nm based on $\epsilon_M = 39,500 \text{ M}^{-1}\text{cm}^{-1}$ as reported by Coon and Lode (11).

Natural and Magnetic Circular Dichroism Measurement

MCD and CD spectra were obtained at room temperature with a specially devised spectropolarimeter (69) with or without a magnetic field of 16 Kgauss using a solution of $0.8 \times 10^{-4} \text{ M}$ Co-Rubredoxin in a cell of 1 cm light path. MCD and CD spectra are additive; hence, all MCD spectra have been corrected for the CD component. Molecular magnetic ellipticity, $[\theta]_M$, is given in units of degree $\text{cm}^2 \text{ dmole}^{-1} \text{ Kgauss}^{-1}$. The solution of CoSO_4 at 0.137 M was used as a standard ($[\theta]_M = 6.2 \times 10^{-3}$ at 510 nm, (70)). Molecular ellipticity for CD spectra, $[\theta]_\lambda$, is given in units of degree $\text{cm}^2 \text{ dmole}^{-1}$. All spectra were corrected using buffer blank in the same cell. CD measurement was also performed with a Durrum-Jasco UV-5 recording spectropolarimeter equipped with a CD accessory.

Laser-Raman Spectra Measurement

The Raman spectrometer was equipped with a Coherent

Radiation CR-5 Ar⁺ laser, a Spex 1401 double monochromator and a cooled RCA C-31034 phototube. Spectra were obtained in rotating cell using transverse laser (4880 Å) excitation.

Difference Spectra Measurement

All spectrophotometric difference measurements were made with Aminco DW-2 spectrophotometer. The base line was recorded by adjusting the multipotentiometers on the spectrophotometer, with an equal volume of buffer in both sample and reference (with split compartment) cuvettes. Equal volume of the rubredoxin and rubredoxin-reductase were then added to the sample cuvette, respectively. The spectrum of a mixture of rubredoxin and rubredoxin reductase, minus that of the separate components, was measured at 25°.

Sulfhydryl Titrations

Aldrithiol-4 (4,4'-dithiodipyridine) and PHMB (p-hydroxymercuribenzoate) were chosen from among the many thiol titrants available. The exact concentrations of reagents were measured spectrophotometrically using $\epsilon_M = 16,300 \text{ M}^{-1}\text{cm}^{-1}$ at 247 nm (71) and $\epsilon_M = 16,900 \text{ M}^{-1}\text{cm}^{-1}$ at 234 nm (72), respectively.

Aldrithiol-4 stock solutions were prepared by dissolving 11 mg of reagent in 0.1 M Tris-Cl at pH 7.3 at 40°. For PHMB, stock solutions were prepared by dissolving 8 mg reagent in 1 ml of 0.04 M NaOH, and diluting the solution to 25 ml with water, then centrifuging to remove particulate material. Prior to use, this stock solution was diluted to the desired

concentration by 0.01 M Na-phosphate buffer at pH 7.0. The PHMB solution was stored at room temperature in the dark.

The number of reactive sulfhydryl groups in the protein was determined by spectrophotometric titration at 324 nm with Aldrithiol-4 using $\Delta\epsilon_M = 19,800 \text{ M}^{-1}\text{cm}^{-1}$ (71) or at 250 nm with PHMB using $\Delta\epsilon_M = 7,600 \text{ M}^{-1}\text{cm}^{-1}$ (73).

For total contents of sulfhydryl groups after metal removal, (2Fe)-rubredoxin suspended in 1.0 ml 5 mM Tris-Cl at pH 7.3 containing 1 mM EDTA, was denatured in situ by the addition of 10 μ l glacial acetic acid. After 10 min. the A_{497} was found to be essentially zero, and the colorless solution was raised to pH 7.5 by the addition of 0.2 ml 1 M Tris base, and the titrant Aldrithiol-4 was added immediately. The same treatment in the reference cuvette containing buffer solution was also carried out. Background absorption from the protein was corrected.

For the time course of the sulfhydryl reactions with these reagents, excess or stoichiometric amounts of Aldrithiol-4 with respect to the protein concentration was added to both reference and sample cuvettes, and the absorption increases were measured with time.

To determine the effect of modification of the available sulfhydryl groups on electron transfer activity, two sulfhydryl groups per mole of Co-rubredoxin were consecutively subjected to PHMB reaction, followed by extensive dialysis against 0.1 M Tris-Cl at pH 7.3 on an UM-10 membrane. The modified Co-

rubredoxin was then assayed by cytochrome c reduction in the presence of reductase and NADH at pH 7.8.

CHAPTER III

RESULTS

Fractions From First DEAE Chromatography (Figure 4 and Table 2)

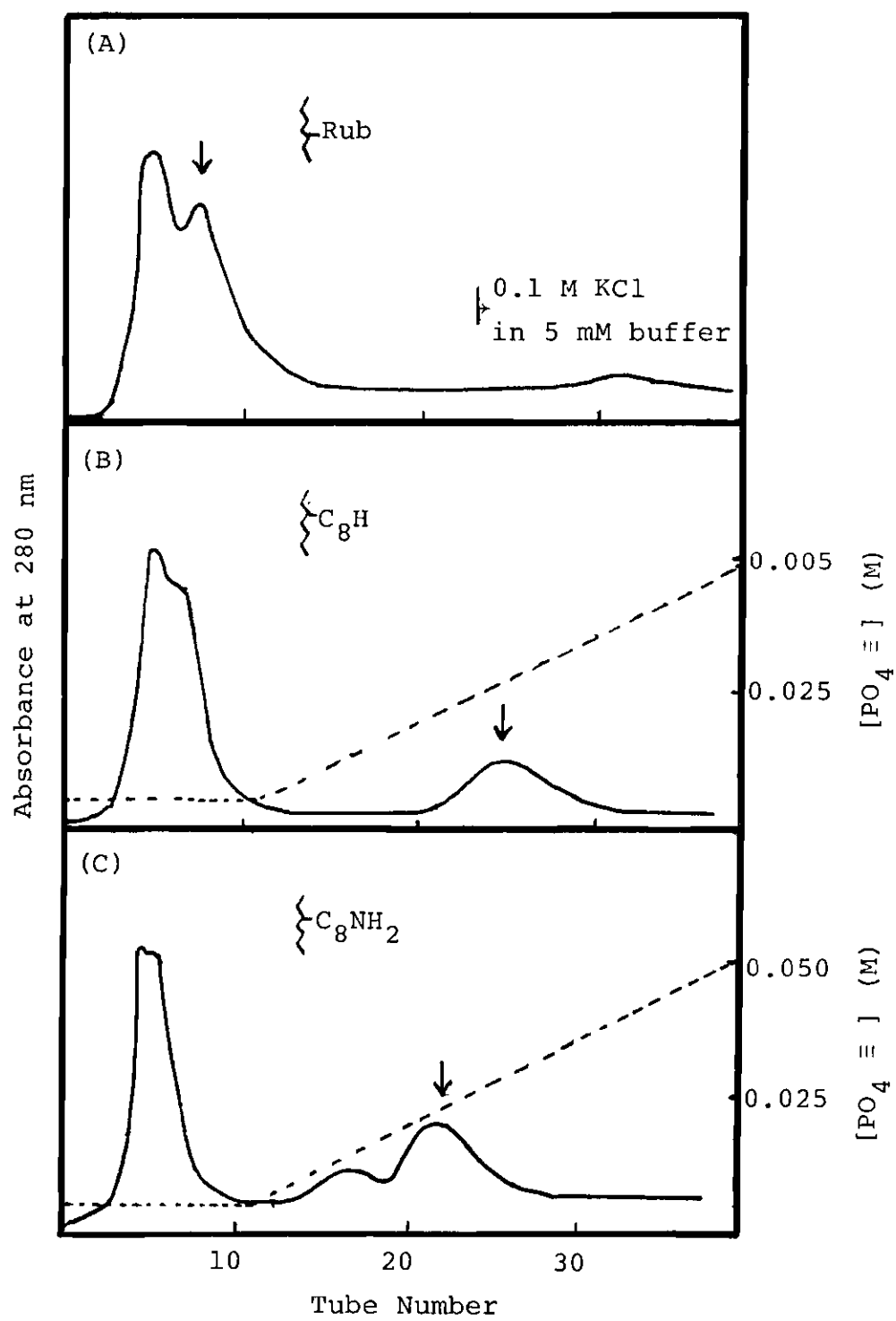
The 30-60% fractionation from ammonium sulfate precipitation contains at least seven kinds of proteins, in addition to rubredoxin. As shown in Table 2, fractions at various eluent concentrations also contain three flavoproteins and three heme-proteins. Interestingly, NADH:rubredoxin reductase was located at fraction 5, as assayed by either cytochrome c reduction or rubredoxin reduction in the presence of NADH. Further purification of this flavoprotein by use of hydrophobic chromatography will be described below. However, none of the heme protein fractions shows the epoxidation activity as assayed by GC, in the presence of rubredoxin, reductase, NADH and lipid (phosphatidyl choline, dipalmitoyl).

Affinity Chromatography of Rubredoxin Reductase

Very little affinity of the reductase for the immobilized rubredoxin was observed as shown in Figure 11A. The reductase eluted essentially as from unmodified Sepharose. Various buffer conditions, including pH change or NADH addition, do not improve the binding activity.

However, the reductase does show some affinity for the alkyl and ω -aminoalkyl Sepharose. The behavior of the reductase in either ω -aminohexyl or ω -aminooctyl Sepharose is essentially

Figure 11. Affinity Chromatography of Rubredoxin Reductase. The crude reductase from the first DEAE chromatography was equilibrated with 5 mM phosphate buffer at pH 7.3, then chromatographed on the following columns, respectively. (A) Immobilized Rubredoxin; (B) Octyl Sepharose; (C) ω -Aminohexyl Sepharose; all preequilibrated with the same buffer. The gradient elution (B and C) was produced by pumping 50 mM phosphate buffer at pH 7.3 into an equal volume of 5 mM phosphate buffer. The arrows indicate where the activity of reductase was found.



the same as shown in Figure 11C. The protein is eluted at 25 mM phosphate buffer, with A_{272}/A_{438} ratio of 7.1. The ability to reduce rubredoxin in the presence of NADH is linear with the concentration of reductase. On the other hand, the reductase with the octyl Sepharose column (Figure 11B) is eluted at 40 mM phosphate buffer, with A_{272}/A_{438} ratio of 10.3.

In experiments described throughout this study, the rubredoxin reductase used was the preparation from either ω -aminohexyl or ω -aminooctyl Sepharose chromatography.

Characteristics of the Isolated Rubredoxin

Using the modified procedure outlined in the Materials section, we obtained rubredoxin with essentially the same characteristics described by Lode and Coon (11). Approximately 140 mg of pure protein was usually obtained from 1 kg of frozen cells, although no attempt was made to maximize the protein yield. As expected, the A_{280}/A_{497} ratio steadily decreased during the course of the purification and the spectral characteristics of the purified protein match those described previously (Table 2 and Figure 11). Disc gel electrophoresis of freshly purified rubredoxin at pH 9.5 gave a single major band after staining but in agreement with Lode and Coon, we also observed a faint slower moving band, which they have suggested may be due to aporubredoxin or denatured protein. Isoelectric focusing experiments were carried out under a variety of different protein and Ampholine concentra-

tions as well as in the presence of the nonionic surfactant, Triton X-100, and of the zwitterionic surfactant, Sulfobetaine DLH. In all cases, severe precipitation and extensive aggregation of the protein occurred. From the final position of the red band, we estimate the pI of rubredoxin to be approximately 4.2, which is not surprising in view of the high content of acidic amino acids in this protein. It seems reasonable to suggest that the extreme insolubility of this protein indicates that it is highly hydrophobic, and this property may play an important role in complex formation with the other components of this enzyme system or with an associated membrane.

Preparation of Immobilized Rubredoxin

In these initial studies, we chose to immobilize rubredoxin on Sepharose 4B since this support has been widely used for the immobilization of many other classes of proteins and other macromolecules. Activation of the support was accomplished using the CNBr method and coupling was carried out at pH 9.5. Preliminary experiments showed that, as expected, coupling at lower pH (8.3) resulted in lower efficiencies of attachment of the protein to the support. Several batches of immobilized rubredoxin were also prepared using commercially available CNBr-activated Sepharose (from Pharmacia). In all cases, care was taken to block any active groups which remained after the rubredoxin coupling through the use of ethanolamine. Glycine is commonly used for this

purpose, but we wanted to avoid the incorporation of additional anionic carboxylate groups into the support.*

Extensive washing with acid, base, high salt and large volumes of buffer were always carried out to remove non-covalently bound material.

Table 5 summarizes representative data on coupling yields of various preparations of immobilized rubredoxin. It is apparent that somewhat higher loadings of immobilized rubredoxin were obtained when commercial CNBr-activated Sepharose (from Pharmacia) was used than when the gel was activated by the procedure of March, et al. (60). However, no attempt was made to optimize the CNBr/gel ratio in our activation procedure, and it is well recognized that this ratio can greatly affect the coupling yield (75). Comparison of preparations III and IV indicate that despite the lower protein/gel ratio, a higher loading was obtained in the latter preparation, and this probably reflects the increased efficiency of coupling at higher pH values (76).

Spectral Properties of Immobilized Rubredoxin

In order to directly examine the spectral properties of immobilized rubredoxin, the conjugate was allowed to gravity settle for at least 3 hours in a semi-micro 10 mm

*It is not generally recognized that the imidocarbonate or isourea linkages formed upon coupling of amino functionalities to CNBr-activated supports impart an often non-negligible degree of positive charge to the conjugate (74).

Table 5. Coupling Yields in Preparation of Immobilized Rubredoxin.

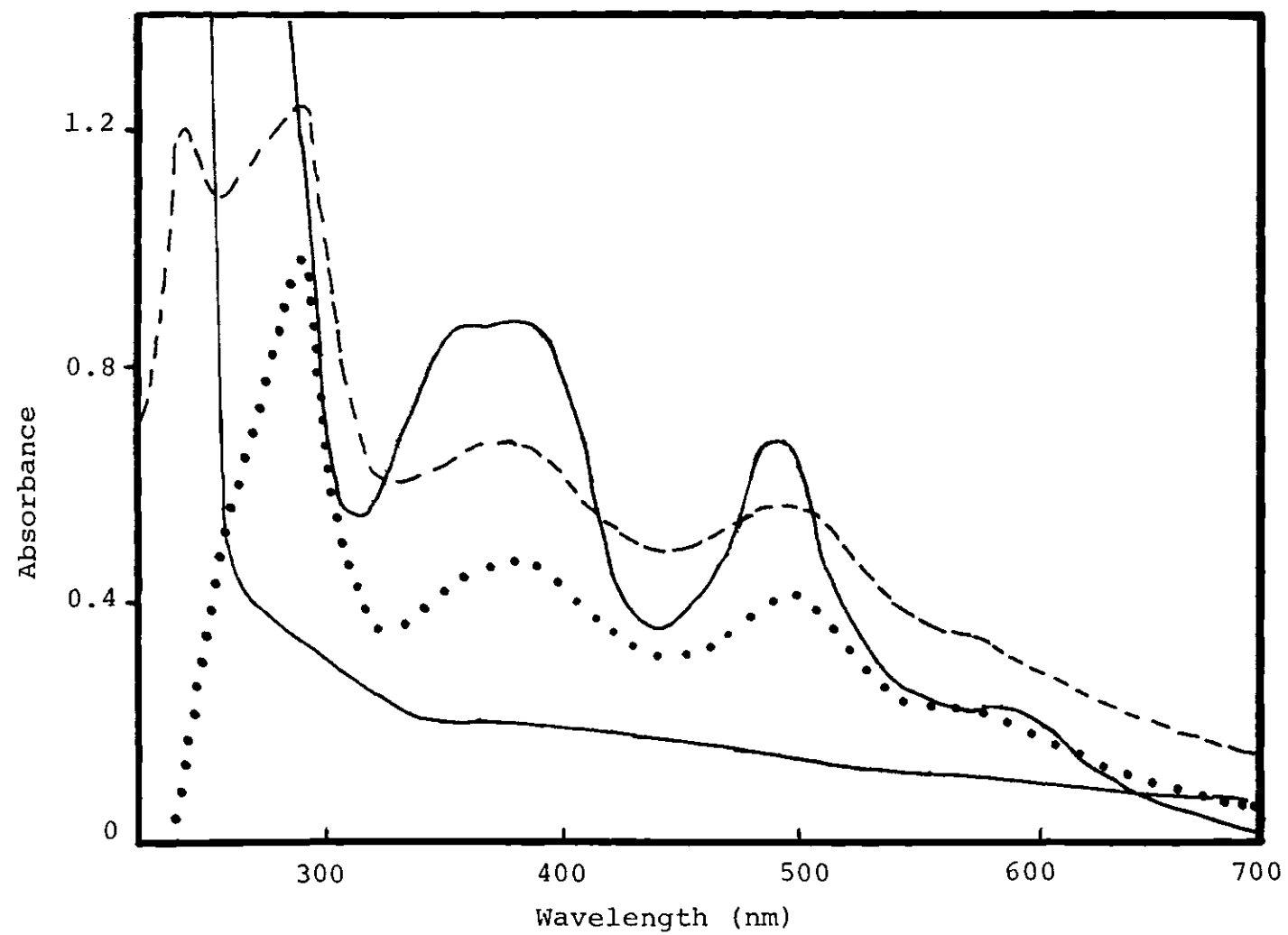
Preparation Number	Activation	Coupling Conditions ^a	A ₄₉₇ Conjugate ^b	mg Enzyme/ g Support ^c
I	March Method ^d	pH 9.5; 36 mg Rubredoxin 20 ml activated gel	0.420	90
II	March Method ^d	pH 9.5; 10 mg Rubredoxin 2.5 ml activated gel	0.520	110
III	Commercial Method	pH 9.0; 16 mg Rubredoxin 1 g lyophilized material ^e	0.750	160
IV	Commercial Method	pH 9.4; 24 mg Rubredoxin 2.5 g lyophilized material ^e	0.909	190

- a. All coupling reactions were carried out at 4° for 20 hrs., followed by reaction with ethanolamine for 2 hrs. at pH 9.0 and 25° to block remaining active groups.
- b. Absorbances were measured after gravity packing in the scattered transmission accessory as described in the Methods section. Reference cell contained CNBr-activated Sepharose.
- c. Calculated based on dry weight equivalent of 27 mg per ml of gravity-packed gel.
- d. Conditions: 200 mg CNBr per ml packed Sepharose.
- e. Commercially supplied lyophilized material was washed with 1 mM HCl before use as suggested by the manufacturer.

path length cuvette. Numerous experiments were carried out to demonstrate that under these conditions, gels of a uniform density are always obtained. A weight equivalent of 27 mg dried gel per ml of gravity-packed material was reproducibly obtained when the gel was dried at 60° or 110° in vacuo, and also when the gel was washed with increasing concentrations of acetone and then dried over P_2O_5 in vacuo at 100° for 20 hrs., in preparation for amino acid analyses. Spectrophotometric measurements were always carried out directly on the gravity packed gels using the scattered transmission accessory of a Beckman ACTA MVI spectrophotometer in order to minimize light scattering effects.

Figure 12 shows comparative spectra of soluble and immobilized rubredoxin. It is evident that the major spectral features of the protein are still evident in the conjugate, with maxima at 497 and 380 nm, and a broad shoulder in the 590 nm region. A slight broadening of the 497 peak is observed in the immobilized conjugate, but the general shape and positions of the minima and shoulders of the spectrum above 400 nm are the same as those observed for the soluble enzyme. On the other hand, a narrowing of the 380 nm peak is observed for the immobilized enzyme, along with a pronounced loss of the shoulder at 360 nm. However, the A_{497}/A_{380} ratios are similar for the soluble and immobilized preparations. It is apparent from the figure that the magnitude of the absorbance of a given preparation of the immobilized enzyme depends

Figure 12. Comparative Spectra of Soluble and Immobilized Rubredoxin. Soluble rubredoxin spectrum (—) was obtained at a protein concentration of 2 mg/ml in 0.1 M Tris-chloride buffer, pH 7.3. Spectra of the rubredoxin-Sepharose conjugate were obtained on gravity-packed gels with the scattered transmission accessory as described in the text, using either Sepharose (---) or CNBr-activated Sepharose (···) in the reference cell. In the latter case, the gel in the reference cell had been washed and treated with ethanolamine after activation exactly as was routinely done during the rubredoxin coupling procedure. The bottom curve is the difference spectrum between CNBr-activated-Sepharose and Sepharose.



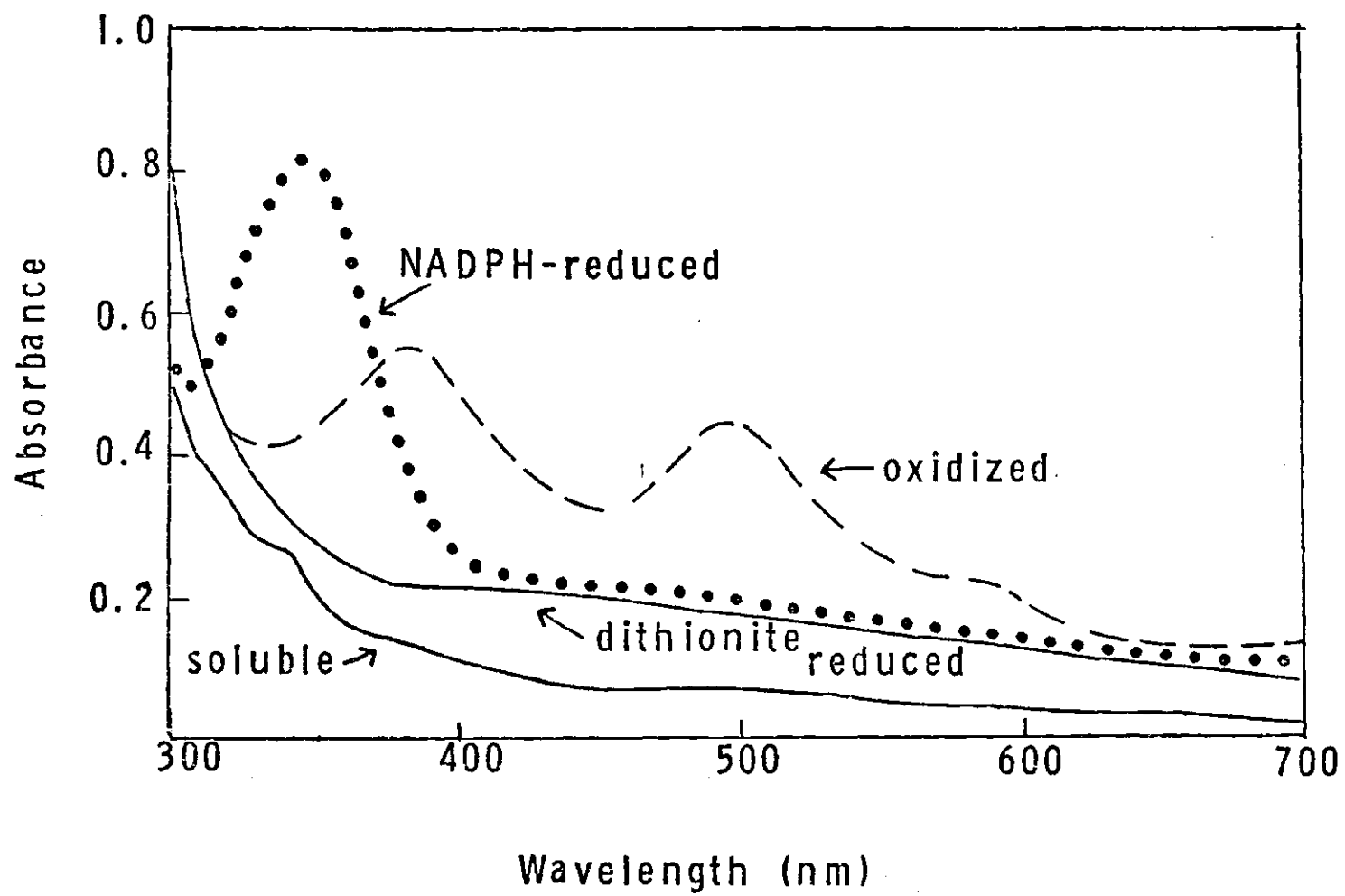
on whether Sepharose or CNBr-activated Sepharose (in both cases gravity packed) is present in the reference cell. In the former case, the spectrum is displaced to higher absorbance, but by an amount equivalent to the optical density difference between CNBr-activated Sepharose and Sepharose. Thus, in subsequent experiments, CNBr-activated Sepharose was routinely employed as the reference material. The region below 300 nm is distorted in the immobilized conjugate; a shift in the 280 nm peak to about 294 nm and a diminution in the size of this peak, along with a new peak at about 240 nm apparently arising from the activated matrix, are evident. The only other report of a direct spectrophotometric measurement on a gravity packed immobilized enzyme conjugate of which we are aware is that of Koelsch, et al. (66). These investigators also reported distortion in the shorter wavelength region, and their immobilized enzyme spectra also show a new peak at 240 nm, but no shift in position of the 280 nm band is apparent in their published spectra. In view of these complications, all quantitative measurements with immobilized rubredoxin were confined to the visible absorption bands. From the known weight equivalent of settled gel and the spectral data on preparation I of Table 5, an "extinction coefficient" at 497 nm of 3,300 was calculated for the immobilized enzyme (based on MW 19,000) which compares with the value of 6,300 reported for the soluble enzyme (11). However, it is not known whether loss of iron from rubredoxin occurs during

the immobilization process, and the total iron binding capacity of the immobilized enzyme may be affected by the activation and coupling conditions employed in the preparation of a particular conjugate (see Discussion Section).

Redox Properties of Immobilized Rubredoxin

To our knowledge, this work represents the first report of the immobilization of an enzyme of this type and we were therefore particularly interested in establishing whether the ability of rubredoxin to accept and transfer electrons, and to interact with other electron-transfer proteins, was altered by the immobilization process. Figure 13 shows comparative spectra for immobilized rubredoxin before and after anaerobic chemical or enzymatic reduction. It is apparent that a bleaching of the visible absorbance of the enzyme, as reported by Peterson and Coon (9) for soluble rubredoxin, is also observed upon reduction of the immobilized enzyme. Anaerobic reduction was also accomplished using spinach ferredoxin-NADP reductase with NADPH as the reducing agent and identical results were obtained (Figure 13). Thus, these experiments establish not only that the immobilized is reducible, but also that it is capable of interacting with, and accepting electrons from, a macromolecular electron transfer protein. Colosimo, et al. (77) have reported that immobilized cytochrome c does not readily transfer electrons to cytochrome oxidase, and steric restrictions by the matrix to the effective interaction of two proteins are not unexpected

Figure 13. Spectral Changes Upon Anaerobic Reduction of Immobilized and Soluble Rubredoxin. Spectra of the rubredoxin-Sepharose conjugate were obtained on gravity-packed gels before and after anaerobic reduction with excess dithionite or excess NADPH in the presence of spinach reductase, as described in the Methods section. For comparison, a spectrum of dithionite-reduced soluble rubredoxin (0.8 mg/ml) is also shown.



with immobilized enzymes (76).

In order to determine whether, once reduced, immobilized rubredoxin can transfer electrons on to another macromolecular acceptor, the rubredoxin-dependent reduction of cytochrome c in the presence of NADPH and spinach reductase (8) was monitored for both soluble and immobilized rubredoxin. Under the conditions of the assay (Figure 14), the reactions were linear with time. In these experiments, the kinetics attachment of the ACTA MVI spectrophotometer, which is equipped with a built-in magnetic stirring system was used. This allows convenient monitoring of the reaction course in a heterogenous reaction mixture of immobilized enzyme and soluble components. The stirring speed is sufficiently rapid to give homogenous mixtures, and the magnetic stirring balls were present in both the sample and reference cells for experiments with both soluble and immobilized rubredoxin.

Figure 14 shows the dependence of the rate of cytochrome c reduction on the amount of rubredoxin present in the reaction mixture. It is apparent that immobilized rubredoxin is indeed capable of mediating electron transfer from the reductase to cytochrome c, although it is less efficient in this role than is soluble rubredoxin. In both cases, the reduction rate is linearly dependent on the amount of rubredoxin present under these conditions. Presumably, the decreased activity of the immobilized enzymes reflects the steric restrictions to interaction with the macromolecular

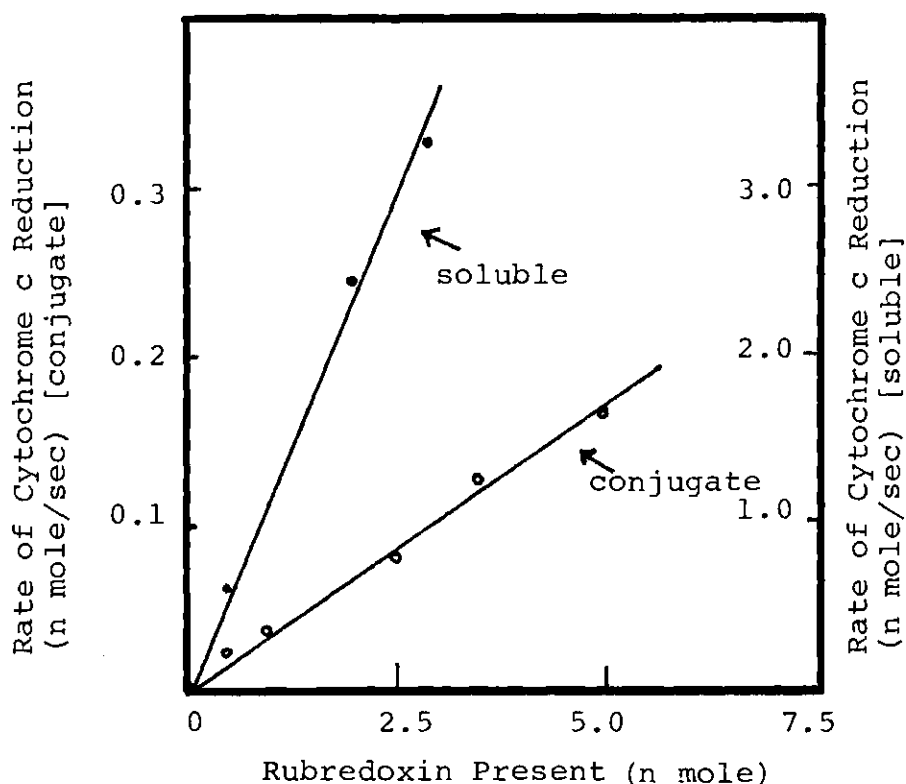


Figure 14. Rubredoxin-Dependent Reduction of Cytochrome c. Varying amounts of soluble rubredoxin or rubredoxin-Sepharose conjugates were added to 25 n mole cytochrome c in 2.0 ml of 0.1 M Tris-chloride, pH 7.8, and the mixtures incubated at 30° for 3 min. Spinach reductase (3.8 μ g) and NADPH (100 n mole) were then added to initiate the reaction. The final volume was 2.06 ml. Cytochrome c reduction was monitored at 550 nm. The rate contributed from the reductase and NADPH was subtracted.

reductant and oxidant presented by the presence of the Sepharose matrix. Similar effects are commonly observed in kinetic studies of immobilized-enzyme-catalyzed processes (for review see (76)).

Having established the ability of immobilized rubredoxin to accept and transfer electrons, we proceeded to determine its reduction potential using the method of Lovenberg and Sobel (34). Typical data obtained in these determinations are presented in Table 6. Assuming a redox potential of -0.116 V for the dye (68), we calculate a redox potential of -0.045 V for immobilized rubredoxin. This compares with a value of -0.037 V for soluble P. oleovorans rubredoxin reported by Peterson and Coon (9), and a value of -0.057 V for soluble rubredoxin from Clostridium pasteurianum reported by Lovenberg and Sobel (34). Thus, it is apparent that the reduction potential of rubredoxin is not substantially altered upon immobilization. It should be emphasized that there are a number of significant operational problems associated with this type of determination with an immobilized enzyme. Among these are (a) possible air leakage into the apparatus during the long settling time, (b) possible lack of complete equilibration between soluble dye and the immobilized enzyme, and (c) a reduction in purging efficiency due to the presence of gel particles in the cell which can easily splatter onto the sides of the apparatus. More than a dozen different redox potential determinations were carried out on immobilized

Table 6. Reduction Potential of Immobilized Rubredoxin.

The data in this table was used with a form of the Nernst equation in calculating the reduction potential as -0.045 V for a one electron transfer.

Conditions	<u>Absorbance</u>		<u>Percent Reduced</u>	
	497 nm	613 nm	Immo. Rub.	Dye ^a
Before NADPH and reductase addition	0.105 ^b	0.246 ^b	0	0
At equilibrium after addition	0.023	0.190	85	12

- a. $E_{m,7}$ for Indigo carmine is -116 mV at 25° .
- b. The absorbance due to the dye and to rubredoxin was 0.01 and 0.95, respectively, at 497 nm, and 0.210 and 0.036, respectively, at 613 nm.

rubredoxin preparations and various degrees of electron "leakage" were observed (compare with reference 34). In all cases, reduction potentials of between -0.045 and -.100 V were calculated for the immobilized enzyme, and thus the conclusion that no gross alteration of the redox potential occurs upon immobilization is certainly warranted. However, the exact value we report here should be considered provisional at the present time.

Guanidine HCl Denaturation of Immobilized and Soluble Rubredoxin

In order to ascertain whether the immobilization process imparts enhanced stability to the tertiary structure of rubredoxin, soluble and immobilized enzymes were incubated in 2.5 M Guanidine HCl and the change in absorbance at 497 nm monitored periodically. As a control, a parallel experiment was carried out on a sample of soluble rubredoxin which had been added to washed Sepharose 4B, but without chemical attachment of the enzyme and support. The results of these experiments are plotted in Figure 15. Since loss of absorbance at this wavelength arises from disruption of the iron chromophore (the apoenzyme has no visible absorbance), it is apparent that this process occurs much less readily in immobilized rubredoxin than in the soluble protein. After 24 hours incubation, the A_{497} of the soluble enzyme had decreased by 90% while that of the immobilized enzyme had decreased by only 20%. While coupling the enzyme to Sepharose increases

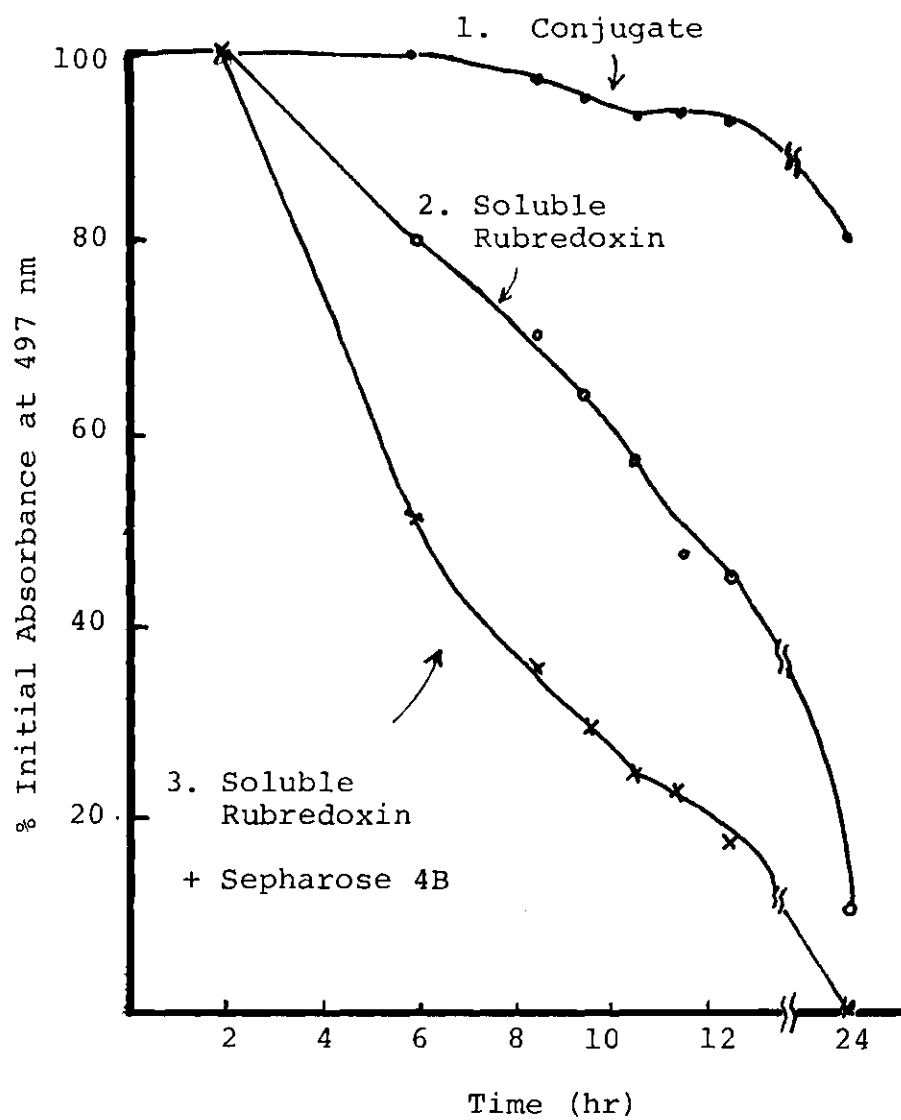


Figure 15. Stability of Soluble and Immobilized Rubredoxin.

its structural stability, the presence of uncoupled Sepharose actually enhances the rate of guanidine HCl denaturation. Although the former effect might be ascribed to multi-point attachment of rubredoxin to the support, the reasons for the latter phenomenon are presently unclear. Data similar to that in Figure 15 were obtained when the absorbance change at 380 nm was monitored, but, as expected, only very small changes in the protein absorbance at 280 nm were observed upon the guanidine HCl treatment.

Iron Removal and Reconstitution of Immobilized Rubredoxin

It was found that the iron was more easily removed from rubredoxin when the iron was in the ferrous state. Therefore, immobilized rubredoxin was converted to the apoenzyme by anaerobic reduction in the presence of excess dithionite, followed by mercaptoethanol washing at high pH. As shown in Table 7, reconstituted conjugate shows approximately the same absorbance at 497 nm as the starting preparation, indicating replacement of the original iron. The entire reduction-apoprotein-reconstitution cycle could be repeated to give the same product obtained after the initial reconstitution. Similarly, incubation of the original preparation under the reconstitution conditions directly, without going through the apoenzyme step, did not result in any increase in the iron content of the conjugate (see Discussion Section).

Table 7. Iron Dissociation and Reconstitution with Immobilized Rubredoxin.

Sample Analyzed	Absorbance at 497 nm ^a
Original Immobilized Rubredoxin Preparation	0.412
After Reduction, Washing and Reconstitution	0.412
After Reduction, Washing and Reconstitution, 2nd Cycle	0.374
Omitting Apoenzyme Step	0.412

a. All measurements on gravity-packed gels.

Reconstitution of Soluble Rubredoxin

Aporubredoxin, obtained by the technique reported here, contains no residual iron, as measured by either atomic absorption spectrometry or electron transfer activity (Table 8; Figure 19). Although native rubredoxin, as isolated, is primarily the (1Fe) species, reconstitution with ferrous ammonium sulfate gives the (2Fe) rubredoxin with spectral properties which are essentially identical to those reported by Lode and Coon (11) using a somewhat different reconstitution procedure. The enzyme is fully active in electron transfer from NADH via the flavoprotein reductase to cytochrome c. Careful reconstitution of aporubredoxin in the presence of approximately stoichiometric (based on binding sites) amount of cobalt salts gives cobalt rubredoxin containing 2 g-atoms of cobalt per molecule of protein (Table 8). Numerous experiments established that reconstitution in the presence of excess cobalt (e.g., 5:1) gives preparations with vastly altered spectral properties, and atomic absorption data with these species indicated variable, non-specific binding of cobalt atoms.

The results of competition studies establish that reconstitution in the presence of mixtures of iron and cobalt salts always results in preferential binding of cobalt over the native iron atom (Table 8). Despite wide variation in the composition of the reconstitution solutions, a consistent total of 2 g-atoms of metal per protein molecule was always

Table 8. Comparison of Iron and Cobalt Binding to Aporubredoxin.

Reconstitution Conditions		Reconstituted Product		
Metal present (g-atom/mol protein)		Metal bound (g-atom/mol protein ^a)		
Co	Fe	Fe	Co	Total metal
0	0 (Apoenzyme)	0	0	0
2	0	0	1.95	1.95
2	0.2	0.25	1.91	2.16
2	1.0	0.67	1.48	2.15
2	2	1.14	1.42	2.56
1	2	1.27	0.91	2.18
0.2	2	1.56	0.13	1.69
0	2	1.90	0	1.90

a. As determined by Atomic Absorption.

obtained, providing additional strong evidence that the cobalt and iron atoms are competing for the same binding site.

Spectral Properties of Cobalt Rubredoxin

The spectral properties of cobalt rubredoxin are fully consistent with the presence of two cobalt atoms in rubredoxin-type binding sites (Figure 16). It exhibits absorption maxima at 350, 470, 620, 685 (splittings), and 748 nm with molar absorptivities (ϵ) at λ_{350} (9405), λ_{470} (3010), λ_{620} (1128), λ_{685} (1232), and λ_{748} (1034), respectively. The intensity and position of the 350 nm band are consistent with charge transfer between Co(II) and thiolate ligands, and are in excellent agreement with those observed in both protein and model systems (ca. 900-1300/Co—S-Cys bond) (50, 78-81). The d-d bands in the visible region are as expected for a distorted tetrahedral high spin Co(II) system.

Natural and Magnetic Circular Dichroism Spectra

While the CD spectrum of the iron species (not shown) is similar to that reported by Peterson and Coon (9), exhibiting a number of strong extrema in the visible region, both positive and negative, the cobalt enzyme exhibits weak extrema at 375 and 348 nm and a positive extremum at 322 nm (Figure 17). The corresponding MCD spectrum exhibits a negative Faraday effect at 350 nm, corresponding to the absorption maximum in the visible spectrum, and a positive Faraday effect at 375 nm. We do not observe any fine structure reflecting the optical

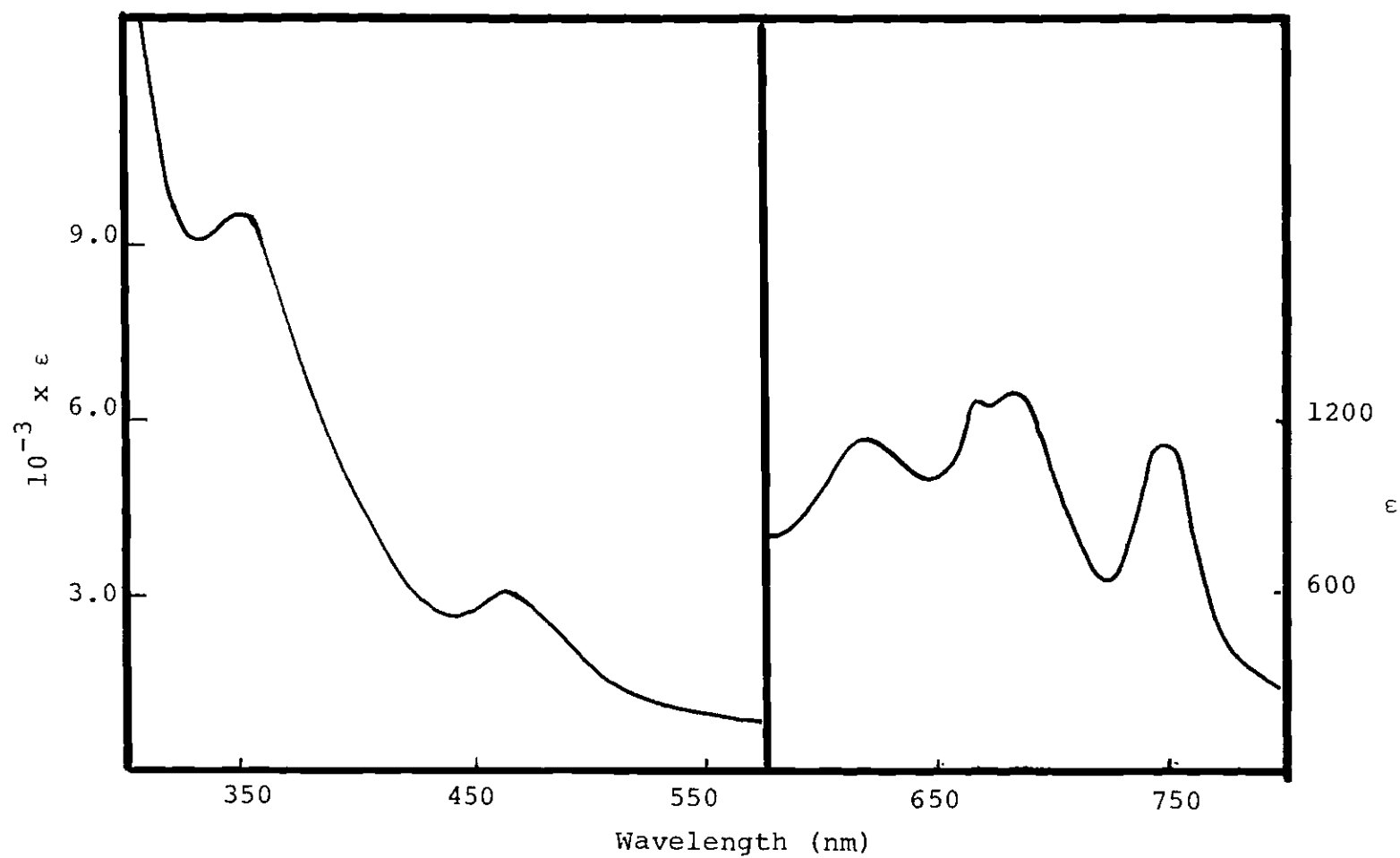
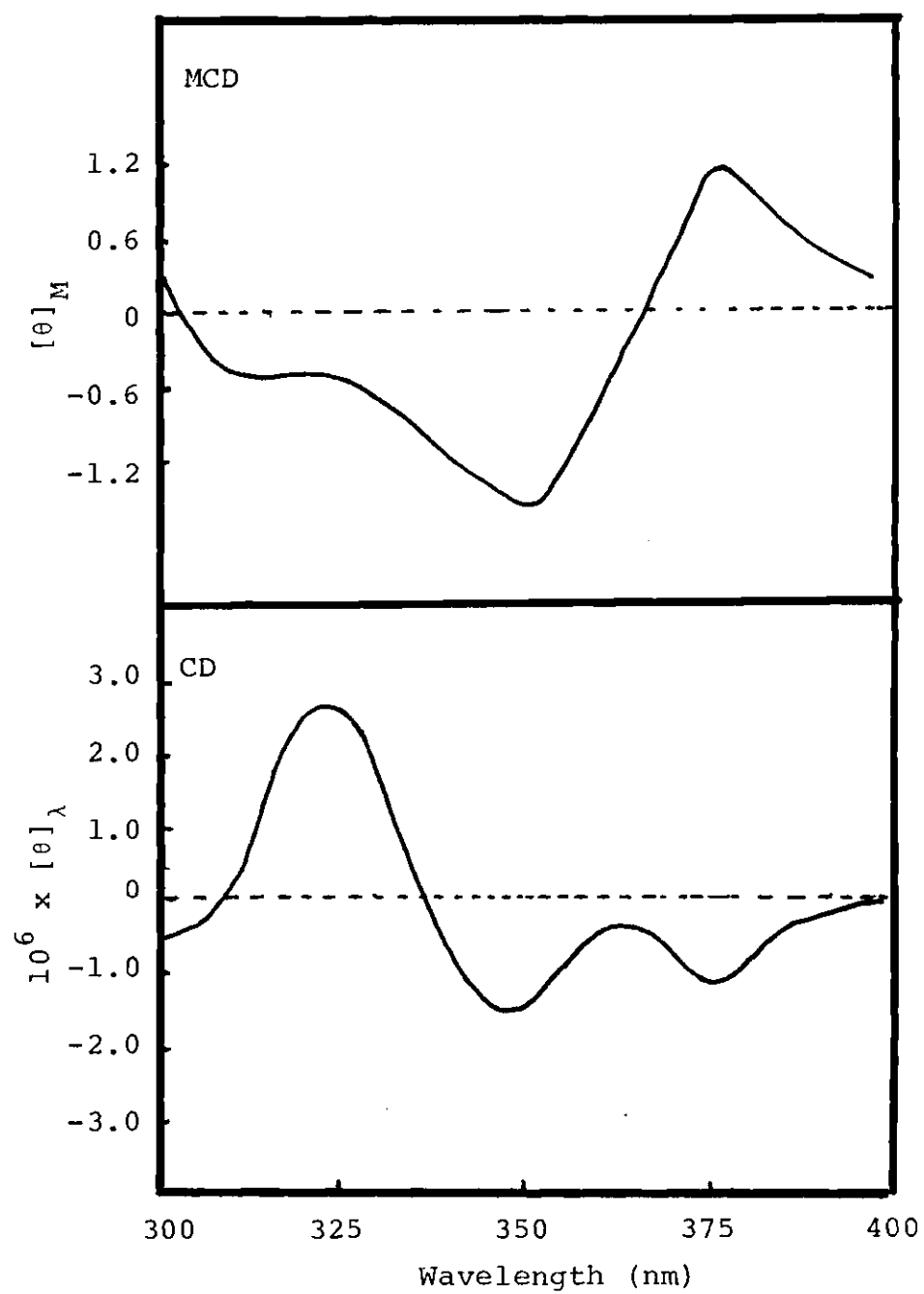


Figure 16. Absorption Spectrum of Cobalt Rubredoxin.
Condition: pH 7.3, 0.05 M Tris buffer at 25°.

Figure 17. MCD and CD Spectra of Cobalt Rubredoxin.
The sample concentration was 8.3×10^{-5} M in
0.05 M Tris-Cl at pH 7.3 with a maximum absorption of 0.78 at 350 nm in a path length of 1 cm.
The natural CD had been subtracted from the total ellipticity in the magnetic field before normalizing to unit field. Sensitivity---10 mV;
time constant---3 sec.; slit---auto; magnetic field---16 KG.



activity in the d-d region, as reported for Co(II) complexes (82).

Laser-Raman Spectra

The resonance Raman spectrum of the cobalt enzyme exhibited only two bands at 419 and 343 cm^{-1} , while we observed bands at 365 and 313 cm^{-1} for (2Fe)-rubredoxin. These latter values are in excellent agreement with the spectrum reported by Long and Loehr (44) for iron-containing clostridial rubredoxin species.

Difference Spectra

Figure 18 shows difference spectra for the interaction of the oxidized forms of both cobalt and iron rubredoxin with NAD:rubredoxin reductase. The spectra were obtained using a split compartment mixing cell in order to allow subtraction of the absorbances of the individual components. It is evident that cobalt rubredoxin interacts with the reductase, with the maxima being shifted somewhat from those which we obtained with the iron enzyme. Also the spectrum shows negative absorption in the d-d region reflecting a possible alteration in the cobalt coordination geometry during the complex formation.

Electron Transfer Activity

Figure 19 shows that cobalt rubredoxin also mediates the reduction of cytochrome c in the presence of the reductance

Figure 18. Difference Spectra of Reductase-Rubredoxin Complex. The spectrum of a mixture of reductase and (2Fe)- or (2Co)-rubredoxin, minus that of the separate components was measured at 25° by the use of a split-compartment cell with a 0.45 cm light path in each compartment. The concentrations were rubredoxin: 3.7×10^{-5} M, and reductase: 3.3×10^{-5} M, in 0.02 M phosphate buffer. The spectra were corrected from the base line, which had been adjusted using the multipotentiometers on the Aminco DW-2 spectrophotometer.

— for cobalt rubredoxin; - - - for iron rubredoxin

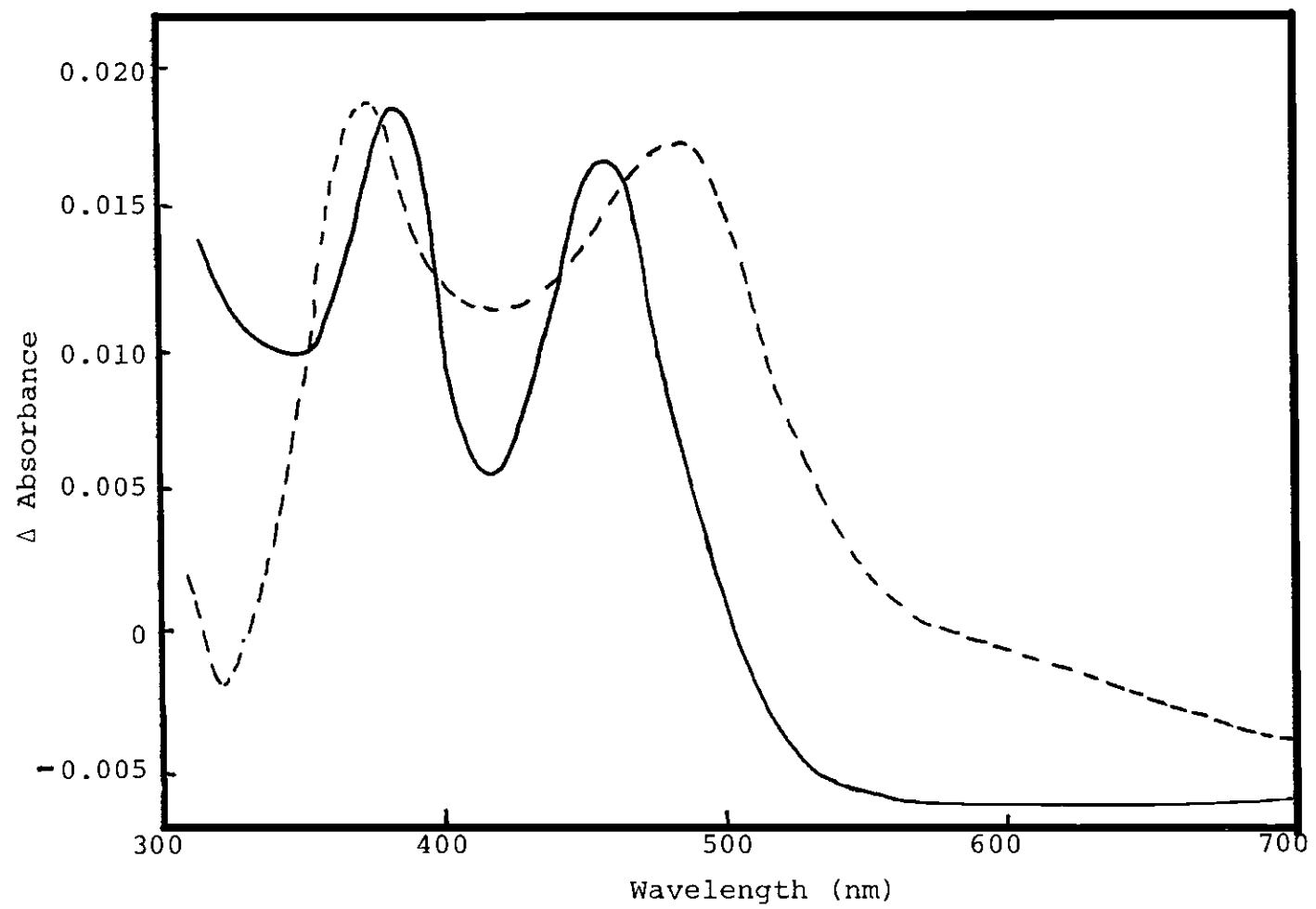
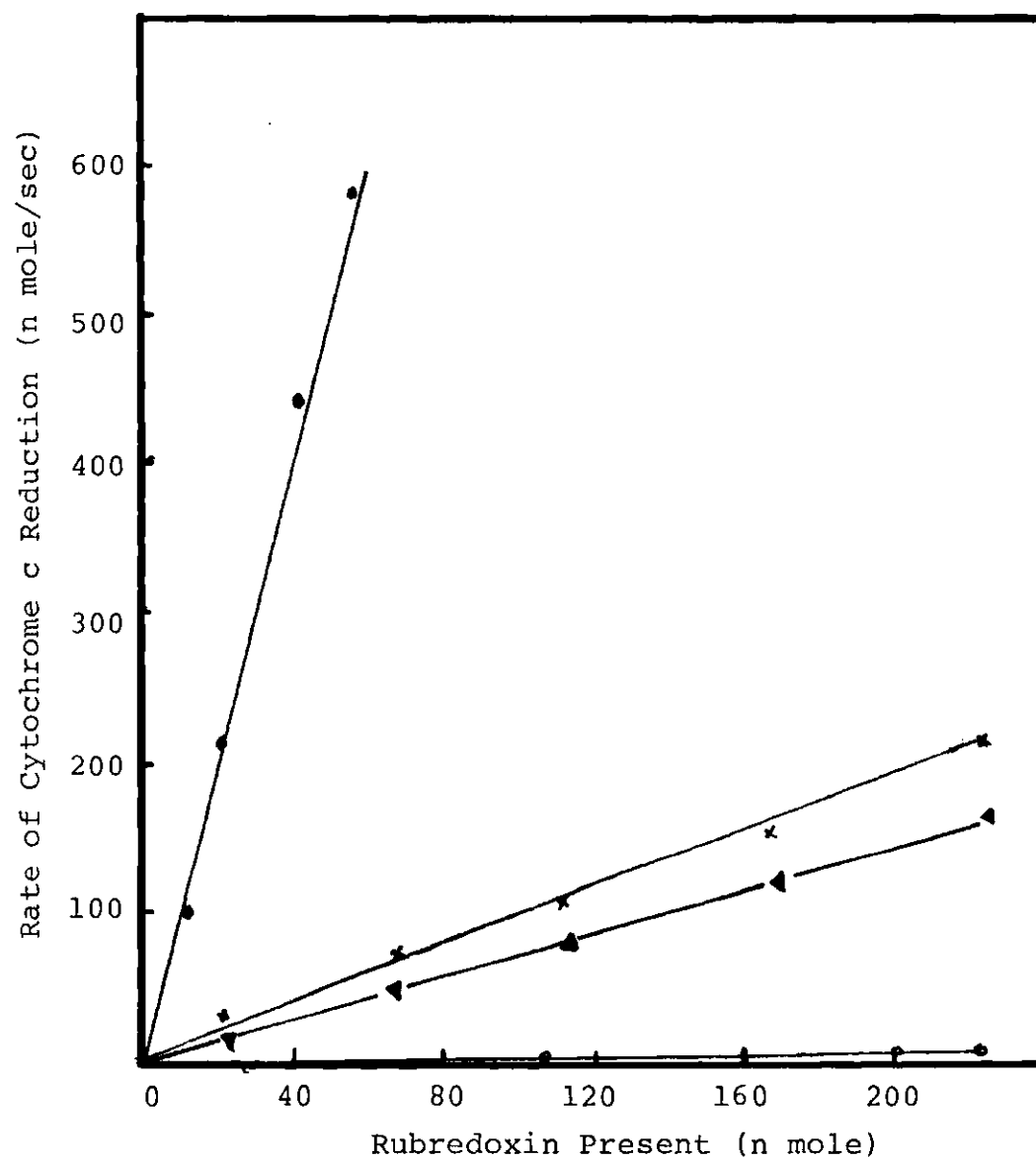


Figure 19. Comparative Electron Transfer Activities of (2Fe)-, (2Co)-, PHMB-Modified Co-, and Apo-Rubredoxin. In each assay, varying amounts of rubredoxin was added to 24 n mole cytochrome c in 1.0 ml of 0.1 M Tris-Cl, pH 7.8, and the mixtures incubated at 30° for 3 min. Rubredoxin-reductase (0.8 μ mole) and NADH (0.28 μ mole) were then added to initiate the reaction. Cytochrome c reduction was monitored at 550 nm using $\Delta\epsilon = 2.1 \times 10^4$. The rate contributed from the reductase and NADH was subtracted. The modified cobalt rubredoxin contained 2 mole PHMB per mole protein.

●—● (2Fe)-rubredoxin;
▲—▲ modified cobalt rubredoxin;
x—x (2Co)-rubredoxin;
o—o aporubredoxin.

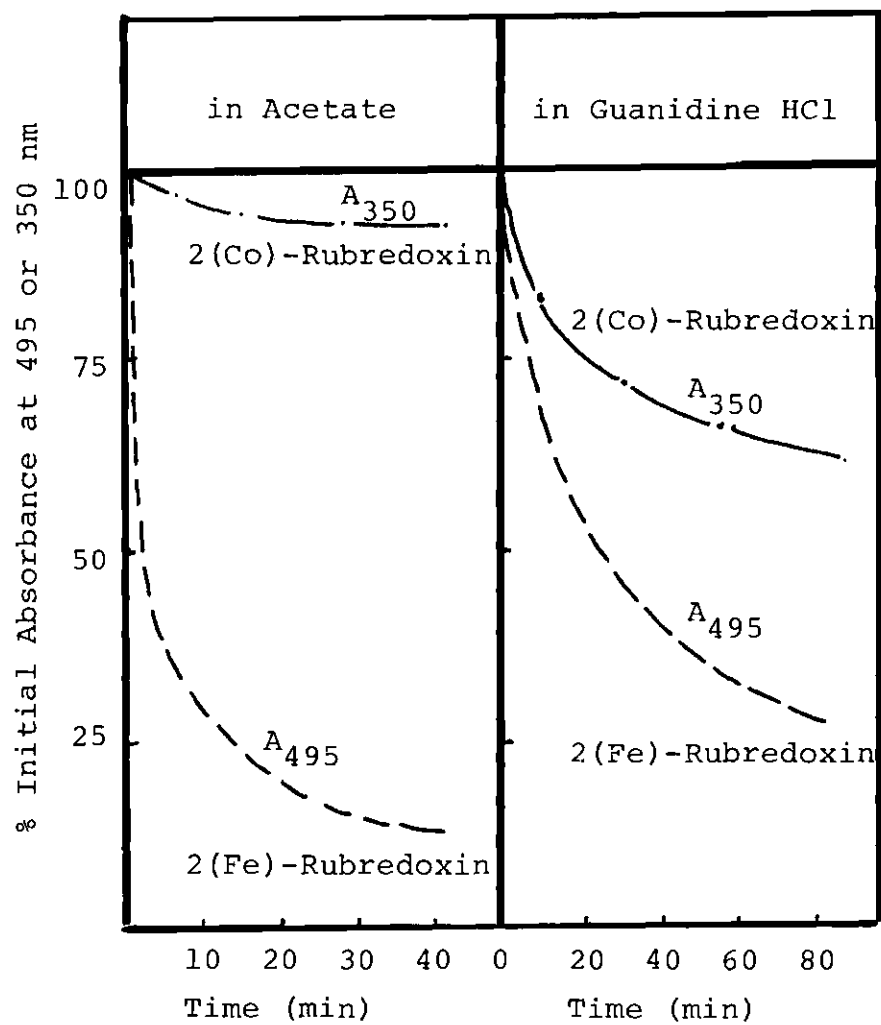


and NADH, although it is less efficient in this role than is iron rubredoxin. Under the conditions of these experiments, the reactions were linear with time, and the rates are linearly dependent on the amount of either rubredoxin species present. For comparison, the activity of aporubredoxin in this concentration range is shown to be negligible, and this establishes a role for the cobalt atom in electron transfer activity.

Stability Toward Chelating and Denaturing Reagents

Native rubredoxin exhibits loss of iron upon prolonged storage, and the "second" iron atom in the (2Fe) species (N-terminal site) is exceedingly labile (11). In sharp contrast, cobalt-rubredoxin (at $A_{350} = 0.35$) exhibits essentially no spectral change at 4° for several weeks. Treatment of (2Fe)-rubredoxin (18 nmoles) with a two fold excess of 1,10-phenanthroline at pH 7.3 results in substantial loss of iron, with spectral change observable within the first few minutes, while under similar conditions only small changes occurred in the d-d region of (2Co) species. Figure 20 illustrates that Co-rubredoxin is also much more stable than the Fe-enzyme toward denaturation in either 6 M guanidine HCl or 0.05 M acid (acetate, pH 3.3). Since loss of absorbance at 495 or 350 nm arises from disruption of the iron or cobalt chromophore, respectively, it is apparent that this process occurs much less readily in cobalt rubredoxin than in the iron enzyme. It is also apparent that, as expected, disruption of iron

Figure 20. Stability Comparison of (2Fe)- and (2Co)-rubredoxin. In separate experiments, each protein (0.07 mg) was added to (A) acetate buffer to give an acetate concentration of 0.05 M at pH 3.3; (b) guanidine HCl gives a guanidine HCl concentration of 6 M at 30°. At the indicated times, absorbance measurement at indicated wavelength were taken for each sample.



chromophores is biphasic, the N-terminal site being vastly more labile even in the absence of denaturants. We have obtained no evidence for a similar non-equivalence of cobalt binding in (2Co)-rubredoxin. As expected, only very small changes in the protein absorbance at 280 nm were observed upon treatment of either the cobalt or iron enzymes with denaturants.

Sulfhydryl Titrations

In our hands, titration of Aporubredoxin which had been prepared in situ from (2Fe)-rubredoxin with Aldrithiol-4 gave reaction of 10 cystein residues, which is consistent with the amino acid composition data (11). In contrast, Lode and Coon (11) reported that at most 8.6 cystein residues could be titrated by Ellman's reagent (DTNB). It is interesting to note that a similar difference between these two reagents towards the thiol groups of urea-denatured thyroglobulin has also been reported (83); Aldrithiol-4 was able to react with thiol groups, which were inaccessible to Ellman's reagent.

The data with CNBr-cleaved rubredoxin (11) support the idea that each of the iron binding sites is composed of four cysteine residues from only one end of the molecule. Since the sequence data (13) establish that a cluster of five sulfhydryl groups exists near each terminus, a single free thiol group is presumably available near each metal binding sites. It has thus been an important goal of a number of investigators to attempt selective modification of these

"extra" sulfhydryl groups in order to probe for a possible role in catalysis or electron transport. However, as the following data indicate, it has not been possible to accomplish this even with (2Fe)-rubredoxin where, presumably, eight of the ten cysteines are involved in metal ligation and might be expected to exhibit diminished reactivity toward sulfhydryl reagents. With (2Fe)-rubredoxin, titration with DTNB (11) resulted in 4 cysteine residues reacting quickly, while at the same time the loss of nearly 50% of the visible chromophore was observed at 575 nm, a wavelength chosen due to the interfering absorbance of the titration product. Our use of Aldrithiol-4 allows one to monitor directly at A_{495} (absorption maximum of protein) during the reaction, since the resultant 4-thiopyridone does not absorb in the visible region. Our titration results with (2Fe)-rubredoxin using this reagent were similar to those reported using DTNB, except that more than 80% of the visible chromophore was lost when the four reactive cysteine residues were titrated (Figure 21). Quantitative addition of PHMB also established that at most 4 sulfhydryl groups can be titrated with the loss of 70% visible chromophore at A_{495} (Figure 22). However, excess amount of PHMB would take a total of six sulfhydryl groups. Taken together, it turns out that the lability of (2Fe)-species might hamper the selective modification of two sulfhydryl groups. Thus in an attempt to investigate this, we turned to (2Co)-species, which was shown more stable in

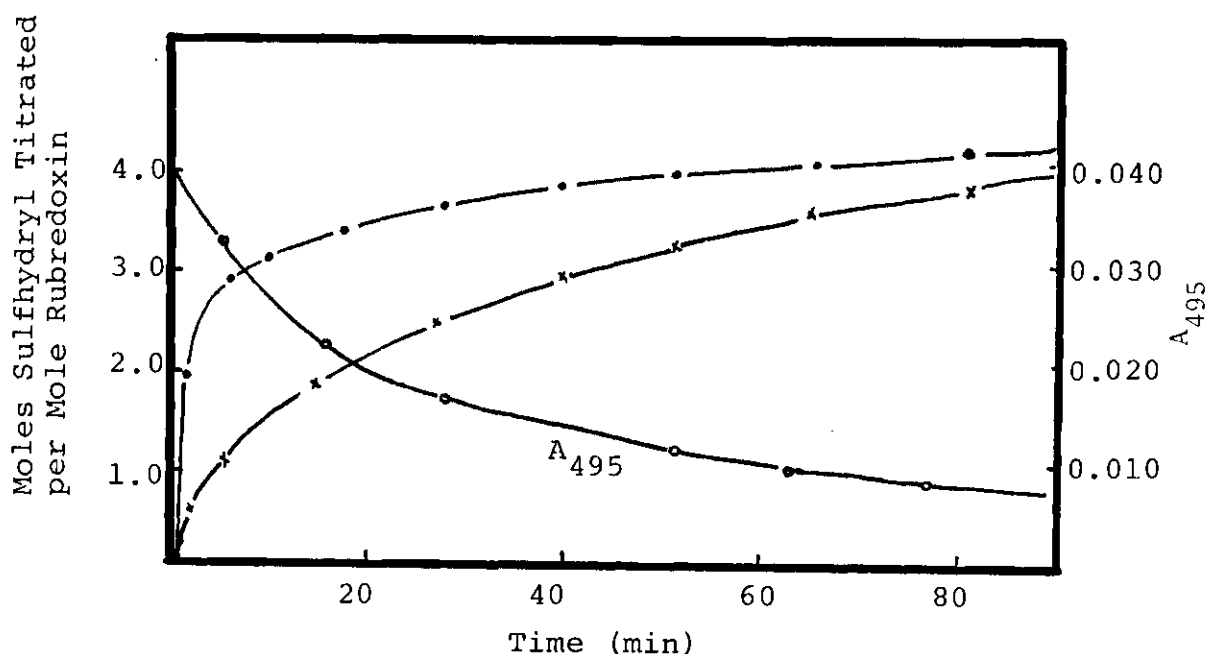
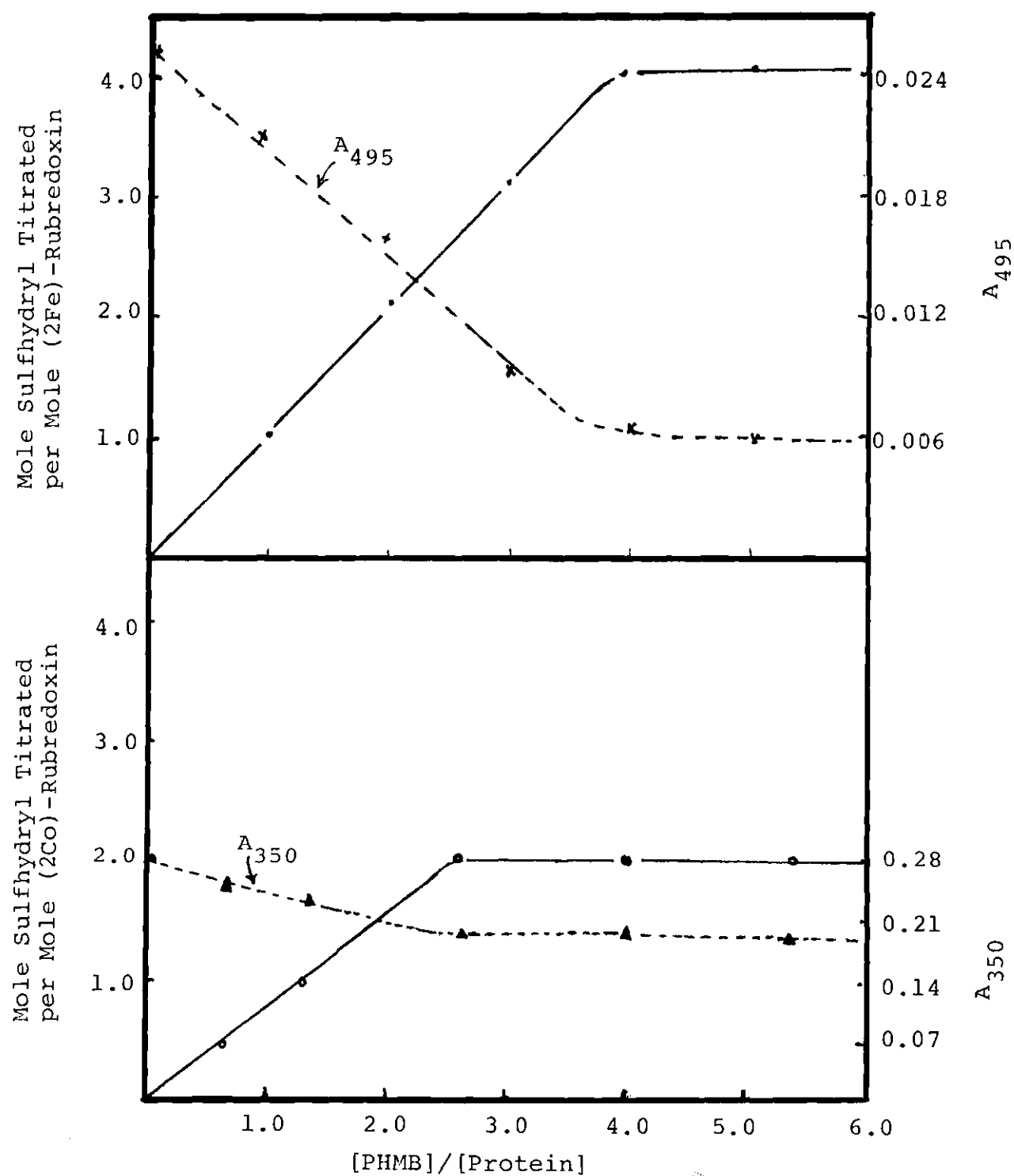


Figure 21. Reaction of Excess Aldrithiol-4 With (2Fe)- and (2Co)-Rubredoxin. Each protein, 4 n mole in 1.0 ml of 0.1 M Tris-Cl, pH 7.3 at room temperature was allowed to react with 25 μ l of 0.05 M Aldrithiol-4. The blank contained 1.0 ml Tris-cl and 25 μ l Aldrithiol-4. The disappearance of iron chromophore was monitored at 495 nm. Very small amount of decreasing at 470 nm was found for (2Co)-rubredoxin. The amount of sulphydryl reacted was calculated from the increase in absorbance at 324 nm.

●—● (2Co)-rubredoxin; x—x (2Fe)-rubredoxin; o—o A₄₉₅

Figure 22. Reaction of Quantitative Amounts of PHMB With (2Fe)- and (2Co)-Rubredoxin. The reactions were carried out in 0.1 M Tris-Cl, pH 7.0, at room temperature. Each addition of the reagents (50 μ l) to both sample and reference (buffer only) cuvetts contained a stoichiometric amount of PHMB with respect to total protein contents. The amount of sulfhydryl reacted was calculated from the increase in absorbance at 250 nm. The disappearance of the chromophores were monitored at 495 nm and 350 nm for (2Fe)- and (2Co)-rubredoxin, respectively.



our work.

With (2Co)-rubredoxin, excess amount of Aldrithiol-4 reacts with 6 sulfhydryl groups in 3.5 hrs., among them two groups which were found to be extremely reactive (within 2 min.) (Figure 21). A time course study (Figure 23) with quantitative addition of Aldrithiol-4 confirmed this finding that two sulfhydryls are more reactive. Strong confirmation for this conclusion also came from titration data with PHMB, which revealed that with PHMB/protein ratios of up to six, only two sulfhydryl groups in the (2Co)-species react vs. four sulfhydryls in the 2Fe)-species (Figure 22). It is thus apparent that with PHMB we have succeeded in establishing conditions under which only two sulfhydryl groups of cobalt rubredoxin react, with alterations of only 25% in the absorbance at 350 nm. The 2Co enzyme with 2 sulfhydryls modified was isolated and assayed for electron transfer activity toward cytochrome c. It exhibited 70% of the activity of unmodified (2Co)-rubredoxin (Figure 19).

Oxidation Reduction Properties of Cobalt Rubredoxin

Essentially identical spectral changes were observed upon the addition of either hydrogen peroxide or *m*-chloroperoxybenzoic acid to Co-rubredoxin, although the latter has a more rapid effect. A fifteen-fold molar excess of hydrogen peroxide (with respect to the cobalt protein) initially doubled the absorption in the d-d region, which was converted

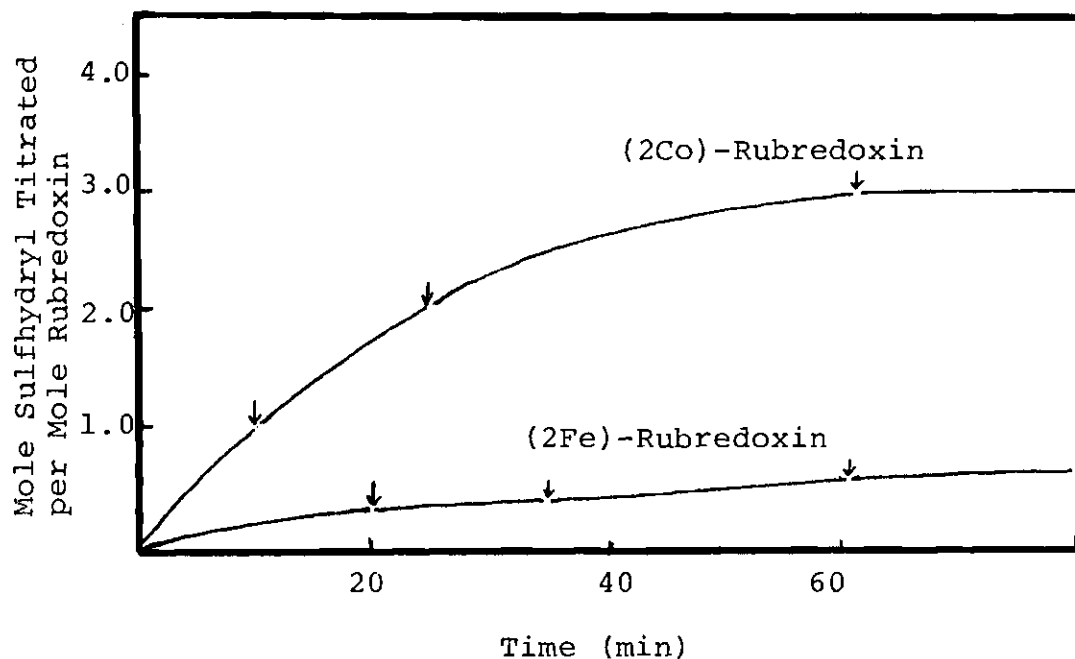


Figure 23. The Time Course of the Reaction with Aldrithiol-4. The condition is the same as described under Figure 21, except that each addition of the reagents allowed only 1 mole-SH/mole protein to react with. The arrows (†) indicate where the reagent added. Overdoses of the reagents to (2Fe)-rubredoxin could not accelerate the reaction.

in 25 min. to a broad peak centered at 670 nm, concomitant with slow disappearance of the 350 nm peak. Then the visible absorption decreased slowly with time with only an observable shoulder at 470 nm. Attempt to reproduce the original spectra by the addition of dithionite to the above mixture were unsuccessful. The addition of hydrogen peroxide to the iron rubredoxin rapidly destroyed its visible absorption bands.

It was also observed that an excess amount of Co(II)-rubredoxin appeared able to reduce cytochrome c slowly, without the participation of reductase and NADH. In an attempt to isolate a possible Co(III)-rubredoxin species, Co(II)-enzyme was incubated with five molar excess of cytochrome c overnight at room temperature. The mixtures were then chromatographed on either CM- or DEAE- cellulose. However, the rubredoxin-containing fractions (breakthrough from CM-cellulose; or 0.2 M KCl in 0.1 M Tris-Cl from DEAE-cellulose) always contained a mixture (with λ_{max} at 410 nm) of oxidized cytochrome c and aporubredoxin, and we were unable to clearly demonstrate the presence of a distinct Co(III)-rubredoxin.

The addition of dithionite crystals or rubredoxin reductase-NADH mixtures to cobalt rubredoxin generally decreases the absorption in the visible region slowly. However, the spectra can be recovered upon prolonged exposure to the air in the former case, but not in the latter case. The 350 nm peak reappeared without changes after dithionite decomposed.

CHAPTER IV

DISCUSSION

Enzymes, the most powerful and specific catalysts known, have discouraged chemists from using them, due to their instability, expense, and scarcity. Circumventing these problems has been the focus of much recent work. The advent of enzyme immobilization has made these problems appear less formidable. Fixing enzymes to supports can be accomplished by four techniques: (1) adsorption onto an insoluble carrier (84); (2) covalent crosslinking of the enzyme into itself or a second type of protein; (3) entrapment within a gel matrix, solid or liquid membrane (85, 86); and, (4) covalent attachment to an insoluble carrier such as glass, agarose, cellulose, dextran or ion-exchange resin (76). Such insolubilization of the enzyme permits its rapid introduction into and separation from a reaction mixture and its reuse. In addition, in a number of cases, immobilization has been found to improve the stability of the enzyme toward denaturation or autolysis, although changes in pH optimum, reaction rate, and substrate specificity upon the immobilization were usually found (87). When proteins are fixed to solid supports, they can no longer readily interact with one another but are able to act on soluble proteins that diffuse to them (88). The immobilized

conjugate, if packed in a column similar to those used in liquid chromatography, can be used as an affinity column for the purification of specific peptides, proteins, or antibodies, provided that the latter recognize the ligand and will be retarded, to an extent determined by the binding constant under the experimental conditions. Those molecules not exhibiting appreciable affinity for the ligand will emerge in the breakthrough volume. Subsequently, the elution of a desired component can be achieved by changing the condition so as to cause dissociation of the interacting species in the column. Parts of this dissertation describe the preparation and properties of the first reported example an immobilized non-heme iron protein on CNBr-activated Sepharose.

Evidently, rubredoxins are the only known proteins containing iron tetrahedrally coordinated by four cysteine-sulfur atoms, which undergo reversible Fe(II)-Fe(III) redox behavior. Replacement of the native metal at the active site of the metalloproteins by other transition metals has proven to be highly useful technique in identifying metal binding groups and in probing for alternations in coordination geometry upon binding of inhibitors and substrate. Cobalt is a particularly useful environmental probe for such purposes due to its paramagnetism and the sensitivity of its visible spectrum, especially in the d-d transition region, to changes in coordination geometry (50, 89-91). Metalloproteins in which the native metal has been replaced by cobalt include carbo-

xypeptidase A, carbonic anhydrase, neutral protease, alkaline phosphatase, yeast alcohol dehydrogenase, yeast aldolase, yeast enolase (for review, see (90)), phosphoglucomutase (92), myoglobin (93), hemoglobin (93), horseradish peroxidase (94), liver alcohol dehydrogenase (79, 81), and stellacyanin (89). Of particular interest in the latter two, which contain one or more sulfur ligands, are the properties of their Co(II) analogs. Studies with the Co(II) analog of stellacyanin confirmed the notion that the intense blue bands of native stellacyanin are attributable to a $\text{Cys-S}^- \rightarrow \text{Cu (II)}$ charge transfer transition (80). The Co(II) complex $[\text{Co}(\text{S}_2\text{-o-xyl})_2]^{2-}$ has recently been prepared and examined spectrally (50) and this well-defined synthetic thiolate complex provides a model for Co(II) in a typical rubredoxin-type metal binding site. Parts of this dissertation describe the first example of a cobalt enzyme chemically (in vitro) reconstituted from a non-heme iron protein.

The effects of immobilization or metal replacement on various properties of rubredoxin, such as absorption characteristics, oxidation-reduction properties and the ability to complex with, and accept electrons from, the reductase were studied. Physical properties such as stability as well as CD, MCD, and laser-Raman spectral properties, were also of concern.

The fact that the immobilized enzyme interacts productively with both spinach reductase (MW 40,000) and cyto-

chrome-c (MW 12,000) in electron transfer processes clearly indicates that the "occupied" iron binding sites are not blocked or rendered completely inaccessible by the presence of the macromolecular support. That the microenvironment of iron is also not significantly altered or distorted in the immobilized state is substantiated by the normal spectral properties and redox potential of the rubredoxin-Sepharose conjugate. It is interesting to compare these findings with the report of Colosimo, et al. (77) that immobilized cytochrome-c on CNBr-activated Sepharose 4B does not transfer electrons readily to cytochrome oxidase and also exhibits a reduced rate of electron transfer to soluble cytochrome-c. It seems likely that steric factors play a role in both of these effects as well as in the reduced efficiency of the rubredoxin conjugates in mediating the reduction of cytochrome-c, and the more radical effect of immobilization on the cytochrome oxidase reaction may be a reflection of the larger steric requirements of this enzyme [MW 90,000 to 200,000 (95)]. However, the specific nature of the interaction between the proteins in question, and the possibility of chemical changes involving amino acid residues directly involved in electron transfer process, e.g., lysines of cytochrome-c (77), must also be considered. It remains to be seen whether electron transfer processes involving other non-heme iron proteins can also effectively operate in the immobilized state.

Upon substitution of the metal, Co(II) rubredoxin also

shows activity, though less than that of the native enzyme. Since the ability to complex with reductase is not altered upon this substitution, as shown in the difference spectrum, it is tempting to speculate that reversible Co(II)-Co(III) redox behavior mimics that of the Fe(II)-Fe(III) system, and is biologically functional. According to this notion, the decreased inferior efficiency of the cobalt enzyme can be attributed to the relatively high redox difference in Co(II)-Co(III) couple, as observed in chemical systems (96). There are several known Co(III)-enzymes including carbonic anhydrase (97), carboxypeptidase A (98, 99), alkaline phosphatase (100) and DNA-dependent RNA polymerase (101). All of these have been obtained from the Co(II) enzymes by hydrogen peroxide or m-chloroperoxybenzoic acid oxidation. In general, although spectral changes concurrent with this valence change are expected, the disappearance of EPR signals inherent to Co(II) (d^7) upon the oxidation is the best experimental probe. Due to short spin-lattice relaxation times, EPR signals of high spin Co(II) complexes are broad and thus such experiments are routinely carried out at liquid helium temperature (102). It must be emphasized that we have obtained no unequivocal evidence for the existence of a Co(III) rubredoxin species after H_2O_2 or m-chloroperoxybenzoic acid oxidation or upon incubation with cytochrome c. Although spectral changes were observed in oxidation experiments, the broad peak centered at 670 nm in the intermediate stage finally vanished. Since

the reductase is positively essential for the electron transfer process, and the cobalt atom does interact with the reductase as shown, the very negative absorption in the d-d regions in difference spectrum, the coordination geometry of the Co(II) may be intrinsically altered by the biological matrix of the complex. Thus, it impairs the efficiency of accepting electrons from NADH. We have also observed that absorption decreases upon dithionite addition, which are reversible after prolonged exposure in the air; similar decreases upon addition of reductase and NADH, on the other hand, are irreversible. Thus, it is also not clear whether a Co(I) intermediate occurs in the electron transfer process. To our knowledge, the Co(I)-S₄ complex has not been described.

Although immobilized rubredoxin is clearly intact and functional, the situation with regard to its total iron content is somewhat unclear. It has been demonstrated that soluble rubredoxin is capable of binding either one or two iron atoms per molecule (11), and while the one-iron form is the species which is actually isolated, Lode and Coon obtained primarily the two-iron form upon reconstitution of the soluble apoenzyme. In contrast, we observe no enhancement in the iron content of the rubredoxin-Sepharose conjugate (as judged from visible absorbance) upon either reconstitution of the immobilized apoenzyme or incubation of the original conjugate under reconstitution conditions. On the other hand, the iron present in the conjugate immediately after immobilization can be both

readily removed under dissociation conditions and virtually completely restored, without difficulty. These results imply that those iron binding sites which are actually occupied during the initial coupling remain substantially intact in the immobilized state, while unoccupied sites either become sufficiently distorted so as to prevent subsequent binding of additional iron after immobilization, or are rendered inaccessible to iron present in free solution in the reconstitution procedure. It is possible that substantial loss of iron from the starting rubredoxin occurs during the coupling reaction itself and thus some rubredoxin molecules may become attached as the apoenzyme. The extent of this loss, and thus the total iron content and iron binding capacity of the conjugate obtained, would be expected to be sensitive to the coupling conditions used for a given preparation. In any case, these considerations should be kept in mind in comparing the operational "extinction coefficient" for the visible absorbance of the immobilized enzyme with that of soluble rubredoxin. No attempt was made to prepare soluble two-iron rubredoxin and then subject this species to immobilization, since the second iron atom is exceedingly labile and is apparently not functional in electron transport (11), the process we were most interested in investigating.

In the case of cobalt rubredoxin, the (2Co) species is always obtained upon reconstitution, and our results establish that this species is considerably more stable than

the corresponding (2Fe) species. However, at the present time, it is not clear whether there are differences in the relative lability and functionality of the two cobalt atoms, similar to the differences observed between the two iron atoms of (2Fe)-rubredoxin. It is known that the metal binding sulfhydryl clusters are located wholly within either end of the molecule—the C-terminal and N-terminal sites, respectively—and the N-terminal iron is vastly more labile and is apparently not functional in the hydroxylation reaction. CNBr cleavage of rubredoxin into two peptide chains, followed by reconstitution to cobalt-containing C- and N- rubredoxin would shed light on this question. However, it should be noted that differences might be expected between the behavior of a metal atom in one of these fragments and its behavior in the complete protein.

The preferential binding of cobalt over the native iron atom to sulfur ligands may be a reflection of either kinetic or thermodynamic factors. It is possible that the color change in reconstitution mixtures before and after the exposure to the air indicates that the initial oxidation states accommodated by the ligands are Fe(II) and Co(I), respectively. However, since the ionic radii of Zn(II) and Co(II) are very close, it remains to be seen whether the former can be accommodated as well. Biosynthetic incorporation of cobalt into the enzyme in vivo might also be feasible, and this technique has been used for yeast alcohol dehydrogenase (78), catechuate 3,4-dioxygenase (103), and DNA-dependent RNA

polymerase (101).

Since we found no evidence for non-equivalence of metal binding in (2Co)-rubredoxin similar to that observed in the (2Fe)-species, the former was employed for the selective modification of sulfhydryl groups. Various data from either Aldrithiol-4 or PHMB titrations confirmed that (2Co)-rubredoxin contains two extremely reactive sulfhydryl groups, which are not distinguishable in (2Fe)-rubredoxin. Subsequent reaction of additional sulfhydryls with thiol reagents requires considerably longer reaction times. It is thus reasonable to assume that the two reactive sulfhydryl groups were not originally participating in metal binding, since we have found the cobalt atom to be quite stable toward dissociation. The inertness of even hydrophobic 1,10-phenanthroline toward the cobalt atoms also supports this notion. However, it should be pointed out that modification of these two reactive sulfhydryl groups by PHMB did result in a decrease of 15% in the charge transfer band concurrent with a 30% loss of electron transfer activity. Based on the ϵ value of 1176/per Co-S-cys bond (see page 75), the removal of two sulfur ligands from a cobalt atom would result in an absorbance decrease of 2352 at 350 nm. However, the observed loss upon modification is 1660, which is much smaller. In our view, the observed decreases in both the charge transfer band and electron transfer activity may well be due to partial unfolding of protein conformation upon the attachment of two large, hydrophobic

p-mercuribenzoate-cysteiny1 residues. An interaction between the proximal cobalt and mercury atoms is also possible. (The d-d transition bands were also decreased.) However, it seems reasonable to conclude that the direct participation of the two free thiol groups in the electron transfer process is not essential, since the activity is not completely lost by the modifications. It would be interesting to determine the effect of sulfhydryl modifications using a rather small methyl group, by reaction with methyl-p-nitrobenzenesulfonate (104, 105). This might circumvent the possible steric complications inherent with the reagents used in this work.

The increased stability of the immobilized enzyme in guanidine-HCl may be at least partially a reflection of tertiary structure stabilization by multipoint attachment of this protein to the matrix. On the basis of studies with model compounds, it is generally assumed that the chemical coupling of proteins to CNBr-activated Sepharose occurs through covalent bond formation between a primary amino groups of the enzyme and the proposed imidocarbonate groups of the activated gel (74-76, 106). There are certainly sufficient lysine residues in rubredoxin to allow these attachments. Since the extent of multipoint attachment possible is dependent on the extent of activation of the gel and the protein loading, optimization of such factors could well lead to highly stabilized rubredoxin conjugates. On the other hand, ligands which bind at the active site (e.g., competitive inhibitors) are often added during the

immobilization of macromolecules to minimize conformational alterations of the active site due to multipoint attachment or direct chemical involvement of active site residues in the coupling reaction, either of which conditions could lead to decreased or altered biological activity (75). It is likely that iron bound to rubredoxin during the immobilization process protects the integrity of the occupied iron binding sites of this enzyme in a similar fashion.

Despite the stability endowed by multipoint attachment, the technique of differential scanning calorimetry has revealed that upon immobilization ribonuclease A becomes fixed in a partly unfolded (inactive) state with restricted flexibility (107). In an attempt to prevent these problems, which may also impair the ability of immobilized rubredoxin to complex with the reductase, the amount of CNBr was decreased in the activation procedure in order to limit the number of imino-carbonate groups available for coupling of rubredoxin and thus minimize multipoint attachment. However, it was found that even with such conjugates, the reductase is only weakly retarded by immobilized rubredoxin. It is possible that for limited point attachment, Sepharose-aminoethyl DTNB (5,5'-dithiobis-(2-nitrobenzoate)) (108), Sepharose-(glutathione-2-pyridyl disulfide) (109), or Sepharose-aminoethyl *p*-chloromercuribenzoate (59), would be suitable for coupling Co-Rubredoxin, via the two available sulfhydryl groups, without affecting the metal binding site. In this approach, the steric restriction

imposed by solid support backbone would also be minimized because the spacer arm would render the rubredoxin exposed to the solvent containing the reductase.

It is worthwhile to reemphasize that the studies on immobilized rubredoxin were greatly facilitated by the ability to directly examine changes in spectral properties on the settled gel. With the use of scattered transmission accessory no serious distortions in the spectra above 300 nm were noted; and particularly with many classes of proteins exhibiting visible absorbance this technique should become very generally useful. The turbidity or opacity of the conjugates usually hampers the direct characterization of their chemical and physiochemical properties. Recent studies on Sepharose-bound proteins have appeared using fluorometry (110), CD (111), and EPR (112), in addition to differential scanning calorimetry previously mentioned.

The spectrum of Co-Rubredoxin between 600 and 800 nm exhibits bands corresponding to the spin-allowed ligand field transitions: ${}^4A_2 \longrightarrow {}^4T_1(P)$. The positions and intensities of these bands are indicative of a distorted tetrahedral high spin Co(II) core (46, 47, 49). Results for Co(II)-S chromophores from available literature data have revealed that cysteinate groups are intrinsically weak-field ligands (50). The intense band at 350 nm is very likely a $S^- \longrightarrow Co(II)$ charge transfer absorption, in excellent accord with those observed in Co(II)-yeast alcohol dehydrogenase, Co(II)-liver

alcohol dehydrogenase, Co(II)-stellacyanin and a well-defined synthetic Co(II)-thiolate complex $[\text{Co}(\text{S}_2\text{-o-xyl})_2]^{2-}$ (50). In each of the above examples, one to four thiolate ligands were coordinated to the cobalt atom. The calculated extinction coefficients were in the range of 900-1300/Co-S-Cys bond. Thus, in the case of Co-rubredoxin, the extinction of 9405 at 350 nm is consistent with the notion that a total of 8 Cys-S groups are involved in coordination of the two cobalt atoms.

The assignment of the absorption band at 470 nm is still uncertain. Tentatively, if this is a charge transfer band and corresponds to the absorption of the iron rubredoxin at 495 nm, while that at 350 nm corresponds to the latter at 365 nm (center), then the energy separation between two charge transfer bands in Co(II) rubredoxin of 7295 cm^{-1} is in good agreement with the 7195 cm^{-1} splitting between two charge transfer band in (2Fe)-rubredoxin. A rough linear correlation between charge transfer band position has been observed for a series of metal ions possessing a given ligand environment (113).

Likewise, the 343 and 419 cm^{-1} Raman bands, which are present in Co(II)-rubredoxin spectrum corresponds to stretching vibrations at 313 and 365 cm^{-1} present in Fe-rubredoxin. The increase in frequency could then be about 40 cm^{-1} for both bands. To our knowledge, our data represent the first set of Raman spectra reflecting Co(II)- S_4 core in a distorted

tetrahedral environment ever reported. The same is true for the MCD data.

The stability of the cobalt chromophore toward 1,10-phenanthroline may arise from whatever environmental effects and precise stereochemical constraints are imposed by the protein structure. The conformation distortion upon cobalt ligation may be arranged in an irregular tetrahedron around the cobalt atom and access of the reagents outside the crevice would seem limited compared with the iron chromophore. The stability constant that may account for the difference between cobalt and iron with sulfur ligands deserves further study. The pair of zinc atoms at a non-catalytic site of liver alcohol dehydrogenase near the surface and coordinated to four S groups donated by four cysteines, was inert to bind 1,10-phenanthroline (81), and this can be accounted for from the thermodynamic considerations. This may also be true for cobalt rubredoxin.

Our experience is that the 30-60% ammonium sulfate fractionation of the sonicate extract contains both rubredoxin and reductase, which are well-separated by DEAE chromatography. It is interesting to note that the amount of reductase is typically at least three times greater than that of rubredoxin. This may indicate that the biological function of reductase is not limited to complexing in a 1:1 ratio with rubredoxin in the oxygenase reaction (hydroxylation or epoxidation). It has recently been found that the reductase

itself also participates in both ketonization of allylic alcohol and hydrogenation of the double bond therein (M. S. Steltenkamp, Ph. D. thesis, Georgia Institute of Technology, 1978). This may represent another important biological function for this flavoprotein.

Preliminary experiments with rubredoxin on alkyl agarose conjugates indicate that the hydrophobicity of this enzyme will allow its purification by using $-C_6$ or $-C_8$ alkyl agarose columns. Increasing ionic strength effectively elutes the rubredoxin. Meanwhile, we are now using ω -aminohexyl agarose to purify the reductase. Likewise, hydrophobic chromatography for the purification of hydroxylase can be expected.

Recently, an immobilized enzyme complex has been prepared and studied as a model for microenvironmental compartmentation in mitochondria (114). It will be interesting to compare the matrix-bound and membrane-bound three enzyme system, composed of rubredoxin, reductase and hydroxylase.

REFERENCES

1. For outstanding recent reviews:
 - (a) Boyer, P. D., (ed.), "The Enzymes," 3rd ed., Vol. 12, Academic Press, N. Y. (1975).
 - (b) Hayaishi, O., (ed.), "Molecular Mechanisms of Oxygen Activation," Academic Press, N. Y. (1974).
 - (c) Gunsalus, I. C., Pederson, T. C., and Rigar, S. G., Annu. Rev. Biochem., 44, 377 (1975).
2. Hayaishi, O., Proceeding of the Planetary Sessions, Int. Congr. Biochem. Abstr. 6th 33, 31 (1964).
3. Guroff, G., Daly, J. W., Jerina, D. M., Renson, J., Witkop, B., and Udenfriend, S., Science 157, 1524 (1967).
4. Hamilton, G. A., J. Am. Chem. Soc., 86 3391 (1964).
5. (a) Hamilton, G. A., Adv. in Enzymol., 32, 55 (1969).
(b) Hamilton, G. A., in Prog. in Bioinorg. Chem., Vol. 1, E. T. Kasier and F. J. Kezdy, editors, Wiley, N. Y., p. 83 (1971).
6. Hamilton, G. A., Annals N. Y. Acad. Sci., 212, 4 (1973).
7. Peterson, J. A., Basu, D., and Coon, M. J., J. Biol. Chem., 241 5162 (1966).
8. Peterson, J. A., Kusunose, M., Kusunose, E., and Coon, M. J., J. Biol. Chem., 242, 4334 (1967).
9. Peterson, J. A., and Coon, M. J., J. Biol. Chem., 243, 329 (1968).
10. McKenna, E. J., and Coon, M. J., J. Biol. Chem., 245, 3882 (1970).
11. Lode, E. T., and Coon, M. J., J. Biol. Chem., 246, 791 (1971).
12. Ueda, T., Lode, E. T., and Coon, M. J., J. Biol. Chem., 247, 2109 (1972).
13. Benson, A., Tomoda, K., Chang, J., Matsueda, G., Lode, E. T.,

- Coon, M. J., and Yasunobu, K. T., Biochem. Biophys. Res. Commun., 42, 640 (1971).
14. Boyer, R. F., Lode, E. T., and Coon, M. J., Biochem. Biophys. Res. Commun., 44, 925 (1971).
 15. Ueda, T., and Coon, M. J., J. Biol. Chem., 247, 5010 (1972).
 16. Reuttinger, R. T., Olson, S. T., Boyer, R. F., and Coon, M. J., Biochem. Biophys. Res. Commun., 57, 1011 (1974).
 17. May, S. W., and Abbott, B. J., Biochem. Biophys. Res. Commun., 48, 1230 (1972).
 18. May, S. W., and Abbott, B. J., J. Biol. Chem., 248, 1725 (1973).
 19. May, S. W., Abbott, B. J., and Felix, A., Biochem. Biophys. Res. Commun., 54, 1540 (1973).
 20. May, S. W., and Abbott, B. J., Abstracts of the 166th National Meeting of the American Chemical Society, Chicago, Ill., Biol. No. 218 (1973).
 21. May, S. W., and Schwartz, R. D., J. Am. Chem. Soc., 96, 4031 (1974).
 22. May, S. W., Abbott, B. J., and Schwartz, R. D., Symposia Preprints, Am. Chem. Soc., 19, 713 (1974).
 23. May, S. W., Schwartz, R. D., Abbott, B. J., and Zaborsky, O. R., Biochem. Biophys. Acta, 403, 245 (1975).
 24. May, S. W., in Catalysis in Organic Syntheses (Rylander P. N., and Greenfield, H., eds.), Academic Press, N. Y., p. 101 (1976).
 25. May, S. W., Steltenkamp, M. S., and Gordon, S. L., Fed. Proceed., 35, 1536 (1976).
 26. May, S. W., Steltenkamp, M. S., Schwartz, R. D., and McCoy, C. J., J. Am. Chem. Soc., 98, 7856 (1977).
 27. Gardini, G., and Jurtshuk, P., J. Biol. Chem., 243, 6070 (1968).
 28. Tyson, C. A., Lipscomb, J. D., and Gunsalus, I. C., J. Biol. Chem., 247, 5777 (1972).
 29. Omura, T., Sanders, E., Estabrook, R. W., Cooper, D. Y., and Rosenthal, O., Arch. Biochem. Biophys., 117, 660 (1966).

30. Scheyer, H., Cooper, D. U., and Rosenthal, O., J. Biol. Chem., 247, 6103 (1972).
31. Lu, A. Y. H., and Coon, M. J., J. Biol. Chem., 243, 1331 (1968).
32. Mason, R., and Zubieta, J. A., Angew. Chem. Int. Edit., 12, 390, and references therein (1973).
33. IUPAC-IUB Commission on Biochem. Nomenclature,
Biochem. Biophys. Arch., 310, 295 (1973).
Arch. Biophys. Biochem., 160, 355 (1974).
34. Lovenberg, W., and Sobel, B. E., Proc. Natl. Acad. Sci., U.S.A., 54, 193 (1965).
35. Lovenberg, W., and Williams, W. M., Biochem., 8, 141 (1969).
36. Benson, A. M., Mower, H. F., and Yasunobu, K. T., Proc. Natl. Acad. Sci., U.S.A., 55, 1532 (1966).
37. Stadtman, T. C., In Non-Heme Iron Proteins: Role in Energy Conversion (A. San Pietro, Ed.) p. 439, Antioch. Press, Yellow Springs, Ohio (1965).
38. Newman, D. J., and Postgate, J. R., Eur. J. Biochem., 7, 45 (1968).
39. LeGall, J., and Dragoni, J. N., Biochem. Biophys. Res. Commun., 23, 145 (1966).
40. Bachmayer, H., Benson, A. M., Yasunobu, K. T., Garrard, W. T., and Whitely, H. R., Biochem., 7, 986 (1968).
41. Boginsky, M. L., and Huennekens, F. M., Biochem. Biophys. Res. Commun., 23, 600 (1966).
42. Mayhew, S. G., and Peel, J. L., Biochem. J., 100, 80p (1966).
43. Watenpaugh, K. D., Sieker, L. C., Herriott, J. R., and Jenson, L. H., Acta. Crystallogr., Sect. B, 29, 943 (1973).
44. Long, II, T. V., and Loehr, T. M., J. Am. Chem. Soc., 92, 6384 (1970).
45. Pivnichny, J. V., and Brintzinger, H. H., Inorg. Chem., 12, 2839 (1973).

46. Davison, A., and Reger, D. L., Inorg. Chem., 10, 1967 (1971).
47. Davison, A., and Switkes, E. S., Inorg. Chem., 10, 837 (1971).
48. Garbett, K., Partridge, G. W., and Williams, R. J. P., Bioinorg. Chem., 1, 309 (1972).
49. Anglin, J. R., and Davison, A., Inorg. Chem., 14, 234 (1975).
50. Lane, R. W., Ibers, J. A., Frankel, R. B., Papaefthymiou, G. C., and Holm, R. H., J. Am. Chem. Soc., 99, 84 (1977).
51. Holm, R. H., Acc. Chem. Res., 10, 427 (1977).
52. Himmelhoch, S. R., Sobel, H. A., Vallee, B. L., Peterson, E. A., and Fuwa, K., Biochem., 5, 2523 (1966).
53. Schwartz, R. D., Appl. Microbiol., 25, 574 (1973).
54. Schwartz, R. D., and McCoy, C. J., Appl. Microbiol., 26, 217 (1973).
55. Schwartz, R. D., and McCoy, C. J., Appl. Env. Microbiol., 21, 78 (1976).
56. Massey, V., Biochem. Biophys. Acta, 37, 310 (1960).
57. Bradford, M. M., Anal. Biochem., 72, 248 (1976).
58. Shin, M., Methods Enzymol., 23, 440 (1970).
59. Cuatrecasas, P., J. Biol. Chem., 245, 3059 (1970).
60. March, S. C., Parikh, I., and Cuatrecasas, P., Anal. Biochem., 60, 149 (1974).
61. Inman, J. K., and Dinitzis, H. M., Biochem., 8, 4074 (1969).
62. Davis, F. J., Annals N. Y. Acad. Sci., 121, 404 (1964).
63. Axén, R., and Ernback, S., Eur. J. Biochem., 18, 351 (1971).
64. Axén, R., Porath, J., and Ernback, S., Nature, 214, 1302 (1967).
65. Zaborsky, O. R., and Ogletree, J., Biochem. Biophys. Acta, 289, 68 (1972).

66. Koelsch, R., Lash, J., Marouardt, I., and Hanson, H., Anal. Biochem., 66, 556 (1975).
67. Sullivan, M. X., Cohen, B., and Clark, W. M., Public Health Report, 38, 1669 (1923).
68. Preisler, P. W., Hill, E. S., Loeffel, R. G., and Shaffer, P. A., J. Am. Chem. Soc., 81, 1991 (1959).
69. Sutherland, J. C., Vickery, L. E., and Klein, M. P., Rev. Sci. Instrum., 45, 1089 (1974).
70. McCaffery, A. J., Stephens, P. J., and Schatz, P. N., Inorg. Chem., 6, 1614 (1967).
71. Grassetti, D. R., and Murray, J. F., Arch. Biochem. Biophys., 119, 41 (1967).
72. Boyer, P. D., J. Am. Chem. Soc., 76, 4331 (1954).
73. Swenson, A. D., and Boyer, P. D., J. Am. Chem. Soc., 79, 2174 (1957).
74. Jost, R., Miron, T., and Wilchek, M., Biochem. Biophys. Acta, 362, 75 (1974).
75. Parikh, I., March, S., and Cuatrecasas, P., Methods Enzymol., 34, 79 (1974).
76. Zaborsky, O. R., Immobilized Enzymes, Chemical Rubber Co. Press, Cleveland (1973).
77. Colosimo, A., Brunori, M., and Antonini, E., Biochem. J., 153, 657 (1976).
78. Curdel, A., and Iwatsubo, M., FEBS Lett., 1, 133 (1968).
79. Drum, D. E., and Vallee, B. L., Biochem. Biophys. Res. Commun., 41, 33 (1970).
80. McMillan, D. R., Holwerda, R. A., and Gray, H. B., Proc. Natl. Acad. Sci. U.S.A., 71, 1339 (1974).
81. Sytkowski, A. J., and Vallee, B. L., Proc. Natl. Acad. Sci. U.S.A., 73, 344 (1976).
82. Kaden, T. A., Holmquist, B., and Vallee, B. L., Biochem. Biophys. Res. Commun., 46, 1654 (1972).
83. Pitt-Rivers, R., and Schwartz, H. L., Biochem. J., 105, 28 c (1967).

84. Messing, R. A., J. Am. Chem. Soc., 91, 2370 (1970).
85. Chang, T. M. S., Artificial Cells, Charles C. Thomas, Publisher, Springfield, Ill., (1972).
86. May, S. W., and Li, N. N., "Biomedical Applications of Immobilized Enzymes and Proteins," 1, 171 (1977).
87. Lasch, J., Bessmertnaya, L., Kozlov, L. U., and Antonov, U. K., Eur. J. Biochem., 63, 591 (1976).
88. Royer, G. P., and Andrews, J. A., J. Biol. Chem., 248, 1807 (1973).
89. Vallee, B. L., and Williams, R. J. P., Proc. Natl. Acad. Sci. U.S.A., 59, 498 (1968).
90. Vallee, B. L., and Wacker, W. E. C., "The Proteins," Vol. 5, (1970).
91. Lindskog, S., "Structure and Bonding," 8, 153 (1970).
92. Ray, Jr., W. J., Goodin, D. S., and Ng, L., Biochem., 11, 2800 (1972).
93. Hoffman, B. M., and Petering, D. H., Proc. Natl. Acad. Sci. U.S.A., 67, 637 (1970).
94. Wang, M. R., and Hoffman, B. M., J. Biol. Chem., 252, 6268 (1977).
95. Caughey, W. S., Wallace, W. J., Volpe, J. A., and Yoshikawa, S., "The Enzymes" (Boyer, P. D., ed.) 3rd ed., 13, 299-344, Academic Press, New York (1976).
96. Cotton, F. A., and Wilkinson, G., "Advanced Inorg. Chem.," 3rd ed. p. 875 (1972).
97. Shinar, H., and Navon, G., Biochem. Biophys. Acta, 334, 471 (1973).
98. Kang, E. P., Storm, C. B., and Carson, F. W., Biochem. Biophys. Res. Commun., 49, 621 (1972).
99. Van Wart, H. E., and Vallee, B. L., Biochem. Biophys. Res. Commun., 75, 732 (1977).
100. Anderson, R. A., and Vallee, B. L., Proc. Natl. Acad. Sci. U.S.A., 72, 394 (1975).
101. Wu, C.-W., Wu, F. Y. -H., and Speckhard, D. C., Biochem., 16, 5449 (1977).

102. Kennedy, F. S., Hill, H. A. O., Kaden, T. A., and Vallee, B. L., Biochem. Biophys. Res. Commun., 48, 1533 (1972).
103. Fujisawa, H., and Uyeda, M., Eur. J. Biochem., 45, 223 (1974).
104. Heinrikson, R. L., Biochem. Biophys. Res. Commun., 41, 967 (1970).
105. Heinrikson, R. L., J. Biol. Chem., 249, 4090 (1971).
106. May, S. W., And Zaborsky, O. R., "Sep. Purif. Methods," 3, 1-86 (1974).
107. Koch-Schmidt A-C., and Mosbach, K., Biochem., 16, 2105 (1977).
108. Lin, L. J., and Foster, J. F., Anal. Biochem., 63, 485 (1975).
109. Brocklehurst, K., Carlsson, J., Kierstan, M. P. J., and Crook, E. M., Biochem. J., 133, 573 (1973).
110. Gabel, D., Steinberg, I. Z., and Katchalski, E., Biochem., 10, 4661 (1971).
111. Zaborsky, O. R., Enzyme Eng. Pap. Res. Rep. Eng. Found. Conf., 2nd, 1973, 161 (1974).
112. Reiner, R., and Siebeneick, M. -U., Enzyme Eng. Pap. Res. Rep. Eng. Found. Conf., 2nd, 1973, 179 (1974).
113. Barnes, J. C., and Day, P., J. Chem. Soc., 3886 (1964).
114. Srere, P. A., Mattiasson, B., and Mosbach, K., Proc. Natl. Acad. Sci. U.S.A., 70, 2534 (1973).

VITA

Jong-Yuan Kuo was born in Kaohsiung, Taiwan on September 8, 1948 and attended elementary and high schools there.

He received the Bachelor of Science Degree in Agricultural Chemistry from the National Taiwan University in 1970. After one year's military service in the Republic of China, he attended the graduate school of Chemistry in the National Taiwan University and worked on the study of snake venoms. In September 1973, he entered the School of Chemistry, Georgia Institute of Technology, graduating with a Ph. D. in Chemistry in January, 1978, under the direction of Dr. S. W. May.

He married the former Alison Ping Yeh on May 7, 1977.